Ultrastructural Analysis of Apoptosis Induced By Zinc Oxide Nanosphere in Human Hepatoma Huh7 Through Mitochondria Dysfunction

Amr Hassan (Amrhassan.nanotechnology@gmail.com)
University of Sadat City
Tamer M.M. Abuamara
Al Azhar University
Emadeldin R. Matar
Al Azhar University
Wael M. Aboulthana
National research center
Hatim A. El- baz
National research center
Mohammad A. Zoair
Al Azhar University
Aly Fahmy Mohamed
Holding Company for vaccine and Sera production (VACSERA)
Ahmed I. Abd El Maksoud
University of Sadat City

Research Article

Keywords: HuH7, Apoptosis, Zinc Oxide Nanosphere, Ultrastructural Analysis, Oxidative Stress, Reactive Oxygen Species, TEM analysis

Posted Date: July 9th, 2021

DOI: https://doi.org/10.21203/rs.3.rs-642242/v1

Abstract

The efficiently of hepatocellular carcinoma therapy predominantly depends on advancement of nanomedicine. Zinc oxide nanostructure is promising material in nanomdicine field due to their unique properties.

Zinc oxide Nanosphere (ZnO Ns) was fabricated with a size 50 nm diameter by a developed Sol-gel approach, using non-toxic biotemplate yeast extract. The physicochemical properties of zinc oxide nanosphere were estimated by Fourier-transform infrared spectrum (FTIR), X-ray diffraction (XRD), dynamic light scattering (DLS), and transmission electron microscope (TEM). Liberated zinc ions released from the zinc oxide nanosphere suspended medium was determined by ICP-AS. The viability was tested by using HuH7 and Vero cells.

ZnO nanosphere was more effectively on cell line than released Zn ions. The cell cycle arrested at G1/S. Also, the apoptosis assay by using Annexin-V/PI showed that apoptosis of HuH7 by ZnO nanosphere is concentration and time-dependent. The mechanism of apoptosis was evaluated via using techniques such as RT-PCR and flow cytometry. The results revealed significance up-regulated of Bax, P53, and Cytochrome C, while a Bcl_2 results displayed significance down-regulated.

Caspase 3 assay results showed that the apoptosis mechanism was intrinsic and extrinsic pathways. Also, ZnO nanosphere and free Zn^{+2} ions induced oxidative stress *via* increasing reactive oxygen species (ROS) and lipid peroxidation. The ultrastructural analysis of HuH7 cell was occurred by TEM.

Transmission electron microscope analysis of HuH_7 after treated with ZnO nanosphere at different times revealed a chromatin condensation of the nuclear periphery fragmentation appearance. Interestingly, the apoptosis of HuH7 cells induced by Zinc oxide nanosphere, showed the canonical ultrastructure features of apoptotic nuclei, and fragmented by budding. Furthermore, There were many vacuoles that filled in the cytoplasm, majority lipid droplets, which resembling those observed in foamy cells, and vesicles with intact membranes, which were recognized as swollen mitochondria.

Introduction

Hepatocellular carcinoma classify as a fifth-most common global malignancy and grade as a third most common cause of cancer-related death in the wide world[1]. Annually, there are more than 600,000 deaths due to Hepatocellular carcinoma[2]. Generally, hepatic cancer (HCC) assort as an aggressive malignancy that diagnosed at end-stage after metastasized[3]. The descriptive Hepatocarcinogenesis is a progressive development of preneoplastic and neoplastic lesions and the acquisition of multiple genetic and epigenetic events contributing to the disease's biochemical/ molecular heterogeneity of the disease[4–5]. Hepatic cancer is prevalent in southern East Asia countries because of the increasing frequency of patients with chronic viral hepatitis. HuH7 is a hepatocyte cell line established in 1982 from a 57-year-old with a well-differentiated hepatocellular carcinoma[6]. HuH7 cells are available in Japan Health Science

Research Resources Bank (catalog number JCRB0403)[7]. It is a better model to investigate the liver toxicity of drugs[1]. In the recent decade, there are many strategies for HCC therapy such as surgery, radiotherapy, and chemotherapy[8]. However, HCC is more resistant to chemotherapy [8–11]. The only treatment for HCC is sorafenib[12]. Recently, there are great developments in the field of HCC therapy[13]. HCC patients who survived after receiving medication are less than 14 percent[14]. The chemotherapy is ineffective in clinical applications because of its side effects[15]. Hence, the development of modern therapeutic agents with better efficiency has been a primacy for HCC remediation[16]. The apoptosis process is a cell death program following well- defines biochemical and morphological characteristics of the apoptotic cells [17–18]. P53 tumor suppressor protein is a powerful caretaker that protects cells from malignant transformation through transcriptional up-regulation of pro-apoptotic DNA repair and cell cycle arrest-related proteins[19]. Nanobiotechnology is the preferable approach to identify a novel, sophisticated therapy[20]. In the last decade, nanomaterials have become a promising approach in medical applications such as cancer diagnosis and therapy. It can be classify as a noble metal and metal oxide material. As well, it classifies as 1 dimension and 2 dimension[20]. Interestingly, there are two pathways to utilize nanoparticles in cancer therapy (passive and active process). The passive processes utilize the enhanced permeability and retention (EPR) effects to enable NPs to diffuse inside and kill- the cancerous cells. Otherwise, inactive processes, Nanoparticles are functionalized and target cancer cells by their conjugation with antibodies or bimolecular receptors, allowing them to target tumor instead of normal cells[21] preferentially. Interestingly, zinc oxide considers as a semiconductor material[22]. The advantages of ZnO nanomaterials are the low toxicity and biodegradability. Their unique properties apply in many applications such as biosensors, catalysts, and cosmetology[23]. A widespread ZnO in sunscreen was approved by the US Food and Drug Administration (FDA), relying on its stability, safety, and intrinsic potential to neutralize UV radiation[24].

Materials And Methods

Chemicals

Zinc acetate hydrate (Zn (O2CCH3)2. 2H2O) was obtained from (Merck, Germany). (India). Yeast extracts were purchased from LOBA Chemical Co. (Mumbai). All aqueous solutions were prepared using milli-Q water (18 M Ω).

Preparation of ZnO nanosphere

The sol-gel method of Bao et al. 2012 with some modifications was used for the synthesis of ZnO-NS[25], where three grams of yeast extract were nurtured to 100 ml ultrapure water and left for one hour. Then, added 25mmol of zinc acetate solution and mixed with 50 ml of yeast extract solution under vigorous stirring for 60 min. followed by thermal treatment at 500 C for 2 hours. The white precipitate obtained was dried and converted into powder to be ready for characterization.

Characterization of ZnO nanosphere

The ZnO nanospheres spectra were assayed by ultraviolet-visible (UV-VIS) spectrometry (JASCO V-630 spectrophotometer, Japan). A Fourier transformed infrared (FT-IR) spectrum of the ZnO nanospheres was characterized *via* the Nicolet 6700 apparatus (Thermo Scientific Inc., USA). The crystalline nature and grain size were analyzed by X-ray powder diffraction (XRD) at a temperature of 25–28 ^{o}C using a D8 Advance X-ray diffractometer (Bruker, Germany) with a nickel (Ni) filter and CuKα (λ = 1.54184 A^{0}) radiations as an X-ray source. The average hydrodynamic size of the ZnO nanosphere in cell culture medium was determined by dynamic light scattering (DLS) (Nano-ZetaSizer-HT, Malvern Instruments, Malvern, UK)[26]. Morphology of the synthesized nanospheres was determined by Field Emission Transmission Electron Microscopy (FETEM) (JSM 2100F, Joel Inc., Tokyo, Japan) at accelerating voltages of 15 and 200 kV, respectively

Measurement of Zn (II) released from ZnO nanospheres.

Quantification a final concentration of released zinc ions from suspended ZnO-NS, the following procures occurred. Firstly, dilution the stock suspension of a concentration of 100 µg/ml ZnO nanospheres by Dulbecco's Modified Eagle's Medium (DMEM) to a final volume of 15ml. Then, incubate all samples at 37 C in a humidified atmosphere (with 5 % CO2) at different times (0, 3, 6,18, and 24 hrs.), .followed by centrifugation for 20 min speed 10,000 x g. then transferring the supernatant (10 ml) into a test tube containing 0.5 ml Conc HNO_3. The solution was filled up to 50 ml with water, and the Zn (II) ions were quantified by using inductively coupled plasma atomic emission spectroscopy (ICP-AES) (Perkin-Elmer, USA) [27–28]

Cell lines

Human hepatocellular carcinoma (HuH7) cells (catalog number JCRB0403) were obtained from Japan Health Science-Research Resources Bank. Green Kidney Monkey (Vero cells) was purchased from ATCC (American Type Culture Collection) (Clone CCL-81). The cells were maintained in a 95% air and 5% CO_2 humidified atmosphere at 37°C. DMEM and MEM-E medium supplemented with 10% FBS and 1% PS were used for routine sub-culturing and all experiments.

Cell viability assay

Determination of the viability of HuH_7 and Vero cell lines occurred via MTT, as described by Mossman[29]. In brief, 1×10^6 cells / well were seeded in 96-well plates and cultured overnight. Different concentrations of suspended Zinc Oxide Nanosphere and $ZnCl_2$ were added to each well for different times. Next, an MTT solution (5 mg/mL) was added to each well for an additional 4 h. The resulting formazan crystals were dissolved in DMSO, and the optical density was measured at 595 nm using an ELX-800n, Multimode Detector (Biotek, USA)

DNA content analysis

The HuH7 cells (3×10^5/well) were seeded into 6-well plates, cultured overnight, and treated with suspended ZnO nanospheres (100 µg/ml) for 24 hrs. The cells were fixed in 75% ethanol at − 4^{o}C

overnight, then incubated with 50 ng/mL PI staining solution and 0.1 mg/mL RNase A in a dark place for 15 min at room temperature. The DNA content of the cells was quantified by flow cytometry (BD FASCCalibur-USA).

Apoptosis Assay with Annexin V-FITC/PI staining

Huh7 cells (3 × 105/well) were seeded into 6-well plates and cultured overnight before exposure to different concentrations of ZnO nanosphere for different times. The cells were then gently collected and incubated with Annexin V-FITC/PI. According to the /manufacturer's protocol, the detection of green fluorescence from Annexin V-FITC and red fluorescence from PI was analyzed using a (BD FASCCalibur-USA[30].

Cell apoptotic mechanisms for RNA extraction and quantitative RT-PCR

The HuH7 cells were cultured in six-well plates and exposed to ZnO nanospheres (100 µg/ml) for 24 hours. At the end of the exposure process, according to manufacture protocol, the extracted RNA concentration was quantitated by using the RNeasy Mini Kit (Qiagen, Valencia CA, USA) [31]. Expressions of p53, Bax, Bcl-2, and cytochrome C genes were quantified using 10 ng of the total RNAs from each sample for cDNA synthesis by reverse transcription using the High Capacity cDNA Reverse Transcriptase kit (Applied Biosystems, USA). The cDNA was subsequently amplified with the Syber Green I PCR Master Kit (Fermentas) in a 48-well plate using the Step One instrument (Applied Biosystems, USA), as a following: 10 min at 95 ºC for enzyme activation followed by 40 cycles of 15 sec at a temperature of 95 ºC, 20 sec at 55 ºC and 30 sec at 72 ºC for the amplification step. Changes in each target gene expression were normalized relative to the mean critical threshold (CT) values of β-actin as a housekeeping gene by the ΔCt method, one µl of both primers specific for each target gene. The specific primer sets for p53, Bax, BCL-2, and cytochrome C are given in table(1). The mRNA levels were quantified using the 2ΔΔCq method. βactin was used as the internal control. Experiments for each gene were conducted in triplicate.

Table (1). the sequence of the oligonucleotide primers used for real-time PCR

Gene name	The sequences of the specific sets of primer
P53	F: 5-TCA GAT CCT AGC GTC GAG CCC-3
	R: 5-GGG TGT GGA ATC AAC CCA CAG-3
Bax	F: 5-ATG GAC GGG TCC GGG GAG CA-3
	R: 5-CCC AGT TGA AGT TGC CGT CA-3
Bcl_2	F: 5-GTG AAC TGG GGG AGG ATT GT-3
	R: 5-GGA GAA ATC AAA CAG AGG CC-3
cytochrome C	R: 5-AAGGGAGGCAAGCACAAGACTG-3
	F: 5-CTCCATCAGTGTATCCTCTCCC-3
βactin	R: 5'GAC CTC ACA GAC TAC CTC AT3'
	F: 5'AGA CAG CAC TGT GTT GGC TA3'

Gene expression by flow cytometry

All flow cytometric analyses were performed on a FACSCalibur flow cytometer (BD, Biosciences, CA, USA). The instrument was aligned and calibrated daily with the use of a 4-color mixture of CaliBRITE beads (BD, Biosciences) with FACSComp Sofware (BD, Biosciences), according to the manufacturer's instructions[32].

The flow cytometry technique evaluated the Bcl-2, Bax, P53, and Cytochrome C oncoproteins. Briefly, after HuH7 Cells were treated with ZnO nanospheres (100 µg/ml) for 24 hrs, cells collected by cold centrifugation at approximately 5000 x g for 10 min then washed twice and re-suspended in 500 µl of cold (+ 4 ^{o}C) 1X PBS buffer containing Triton X-100 (permeabilization step). After centrifugation as previously described, the supernatant was removed, and the pellet has been re-suspended again in PBS containing BSA (1%) and diluted primary antibody rabbit monoclonal antibody (1:100) (Oncogene, Cambridge, MA, USA) for P_{53}, Bax, Bcl2 and cytochrome C. followed by incubation at room temperature for 1hr. After centrifugation, the pellet has been washed three times using PBS, and the cells were incubated with secondary antibodies, anti-rabbit (all from Santa Cruz Biotechnology, USA) in dilution of 1:100 followed by incubation in the dark for 30 min at RT. Finally, the cells were centrifuged, and the supernatant was removed, then the cells have been washed as previously described. The pellet was finally re-suspended in 500 µl PBS. The cells were immediately analyzed by flow cytometry (BD FASCCalibur-USA) [32].

Caspase-3 assay

A standard fluorometric microplate assay determined the activity of the caspase-3 enzyme[33]. Briefly, HuH7 cells (1×10^4 cell/well) were cultured in a 96-well plate and exposed to ZnO nanosphere at the concentrations of 50,100, and 150 µg/mL for 24 hrs. After the exposure was complete, cells were harvested in ice-cold PBS for preparing cell lysate. Further, a reaction mixture containing 30 µL of cell

lysate, 20 µL of Ac-DEVDAFC (caspase-3 substrate), and 150 µL of protease reaction buffer (50 mM HEPES, 1 mM EDTA, and 1 mM DTT) (pH 7.2) was incubated for 15 min. Fluorescence of the reaction mixture was measured at 5-minute intervals for 15 minutes at excitation/emission wavelengths of 430/535 nm using an ELISA reader apparatus (ELX-800n, Biotek, USA). The 7-amido-4- tri-fluoro-methyl coumarin (AFC) standard ranging from 5 Mm to 15 µM was prepared, and its fluorescence was recorded to calculate caspase-3 activity in terms of pmol AFC released/minute/mg protein.

Oxidative stress and antioxidant biomarkers

The HuH7 cells were exposed to different ZnO nanospheres and free Zn^{+2} ion (release from 100 µg/ml ZnO-nanosphere) for 24 hrs. After the exposure, the cells were washed and harvested in cold PBS at 4°C. The harvested cell pellets were lysed using a cell lysis buffer [20 mM Tris-HCl (pH 7.5), 150 mM NaCl, 1 mM Na_2EDTA, Triton X 100 (1% v/v) and 2.5 mM sodium pyrophosphate]. After cold centrifugation at 15,000 g for 10 min, the supernatant (cell extract) was maintained on ice until assayed for oxidative-stress biomarkers. The extent of membrane lipid peroxidation (LPO) was estimated by quantifying malondialdehyde (MDA) [34]. MDA is one of the final products of membrane LPO. In brief, 0.1 ml cell extract mixed with 1.9 ml of 0.1 M sodium phosphate buffer (pH 7.4) then incubated at a temperature of 37°C for 1hr. After precipitation with trichloroacetic acid (TCA) (5% v/v), then incubated mixture was centrifuged (2300 g for 15 min at room temperature). The supernatant was collected and to which 1 ml of TBA (1% v/v) was added and placed in boiling water for 15 min. After cooling to room temperature, the absorbance of the mixture was taken at a wavelength of 532 nm and converted to nmol/mg protein using the molar extinction coefficient of $1.56\times105\ M^{-1}\ Cm^{-1}$.

The level of the reduced glutathione (GSH) was estimated using Ellman's reagent[35]. The reaction was monitored at a wavelength of 412 nm, and the amount of GSH was expressed in nmol/mg protein. Also, nitric oxide (NO) level was measured by determining total nitrate and nitrite concentrations in a sample using the method reported by Green *et al*. (1982)[36].

After exposure of HuH7 cells to ZnO nanospheres (100 µg/ml), the sample is collected and centrifuged at 1,000 g for 20 min to remove particulates, followed by collecting pellet and consecutive washing with PBS (0.02 mol/l at pH 7.0 ± 0.2) to be used for determination of Reactive Oxygen Species (ROS) by kit (Life Span Bioscience Inc., Seattle, WA, USA). All reagents were prepared by adding 100 µl of a sample, standard and blank for each well, followed by incubation at 37°C for 90 min. All samples were then aspirated, and 100 µl of biotinylated detection antibody was added to the pellet and incubated for 1 hr (37°C). After centrifugation (3,000 g), the supernatants were aspirated, and the pellets were washed three times by adding 100 µl of HRP conjugate, followed by incubation at 37°C for 30 min. The supernatants were removed by aspiration and washed five times before adding 90 µl of TMB substrate solution and incubating at 37°C for 15 min. The reaction was stopped by adding 50 µl of stop solution, and then the absorbance of the medium was measured immediately at a wavelength of 450 nm.

Superoxide dismutase (SOD) assay is a mixture containing sodium pyrophosphate buffer, nitro blue tetrazolium (NBT), phenazine methosulphate (PMS), reduced nicotinamide adenine dinucleotide (NADH), and the required volume of cell extract. One unit of SOD enzyme activity is defined as the amount of enzyme required to inhibit chromogen production (optical density at 560 nm) by 50% in 1 minute under assay conditions and expressed as specific activity in units/mg protein[37].

Morphological of apoptosis

To investigation the total fraction of cell with a fragment nucleus among the total count of cell population was taken place by using hematoxylin-stained slides. Also, study the apoptotic process for Huh7 occurred[18].

Ultrastructure of HuH7 using a transmission electron microscope

The HuH7 cells were remedied to ZnO nanosphere at concentration 100 µg/ml for different time intervals. After the end of exposure, cells were harvested and washed with PBS then fixed in ice-cold glutaraldehyde (2.5%) for one hour. The cells were washed with PBS three times for 15 min and post-fixed in OsO_4 (1%) for one hour, then stained with uranyl acetate (2%) for 30 min at room temperature. The cells were dehydrated through serial dilutions of ethanol (50, 70, and 90%) for 15 min each. The dehydration followed this in ethanol (100%) for 20 min and acetone (100%) for 20 min, respectively, and then embedded in Epon812. Ultrathin sections (120 nm) were obtained and stained with uranyl acetate (2%) for 20 min, and lead citrate for 5 min then examined using Field Emission Transmission Electron Microscopy (FETEM) (JSM 2100F, Joel Inc., Tokyo, Japan) at accelerating voltages of 15 kV and 200 kV, respectively [18].

Results

Characterization of ZnO nanospheres

As shown in supplement Fig.s1, the UV-visible spectrum exhibits a sharp rise in absorbance at a wavelength of 359 nm, which identifies the ZnO nanosphere. Figure 1 illustrated the FT-IR spectra of the ZnO nanosphere. There is a band at 3,429 cm^{-1} correspondings to the hydroxyl group of a water molecule on the surface ZnO nanospheres and occurred as a result of the ZnO-Nanosphere's thermal treatment at 500°C. The band at 1,628 cm^{-1} is related to the OH bend to ZnO. Also, a strong band at 418 cm^{-1} was attributed to ZnO. As illustrated in Fig. 2, the XRD patterns of ZnO nanospheres showed that the peaks at 2 θ = 31.746, 34.395, 36.226, 47.526, 56.549, 62.832, 67.893 and 69.028 were assigned to (100), (002), (101), (110), (103), (200), (112) and (201) of ZnO nanosphere. All peaks are consistent with a polycrystalline Wurtzite structure (Zincite, JCPDS no.: 89-1397). There are no characteristic peaks of any impurities, and this indicated a high ZnO nanosphere quality. Scherer's equation estimated the average of the crystallite size (d) of ZnO nanospheres to be of ca. 50 nm. DLS determined the average

hydrodynamic size of ZnO nanosphere in cell culture media, and it was about 149 nm as revealed in Fig. 3 and Supplement Fig. 2.

$d = k\lambda / \beta \cos \theta$

As Fig. 4 and Supplement Fig. 2 showed, TEM images confirmed that the morphological shape of the nanosphere with approximately size of – 50 nm. Also, it was similar to the data obtained by XRD.

Measurement of Zn (II) released from ZnO nanospheres.

ICP-AES measured quantity of the Zn (II) ions released in the supernatant of the dispersed ZnO nanosphere (100 µg/ml). As presented in Fig. 5, the total amount of ZnO nanosphere varied within different interval times. Values of the free Zn^{+2} ions were about 20 after 24 hrs, 15 after 18 hrs, 10 after 12 hrs, 6.5 after 6 hrs, 3.5 after 3 hrs and 1.0 ppm after 1hr.

Cell viability by MTT assay

MTT assay is the best technique to measure of the cytotoxicity of ZnO nanosphere and $ZnCl_2$, to evaluate the activity of Zn ions, on The Human hepatocellular carcinoma (HuH7) and Green Kidney Monkey cell lines (Vero). As Fig. 6A displayed, the viability of HuH7 cells decreased from 100 percent at 0.5 µg to be less than 10 and 15 percent (for ZnO –Ns and $ZnCl_2$ respectively) after treated with of 100 µg (ZnO nanospheres and $ZnCl_2$ respectively) for 24 hours. Similarly, as Fig. 6B demonstrated, the viability of HuH7 cells after treatment for 48 hours reduced from 100 percent to be 20 and 15 percent for ZnO –Ns and $ZnCl_2$ respectively .

The viability of Vero cells was affected less than HuH7 when exposed to both ZnO nanospheres and $ZnCl_2$.As Fig. 6C displayed, the viability of Vero cells decreased from 100 percent at 0.25 µg of ZnO nanospheres and $ZnCl_2$ respectively to be less than 15 and 10 percent (for ZnO –Ns and $ZnCl_2$ respectively) after treated with of 250 µg of ZnO nanospheres and $ZnCl_2$ respectively for 24 hours. Similarly, the viability of Vero cells after treatment for 48 hours reduced from 100 percent to be 20 and 15 percent for ZnO –Ns and $ZnCl_2$ respectively. As Fig. 6D shown, the results changed gradually after exposure of Vero cells to ZnO nanospheres and $ZnCl_2$ for 48 hrs. The viability of the Vero cell decreased from 100 % percent at 0.25 µg of ZnO nanospheres and $ZnCl_2$ to less than 10 % at 125 µg of ZnO nanospheres and $ZnCl_2$.

DNA content analysis

Measurement of the cell cycle phase ratio using flow cytometry with propidium iodide (PI) staining in order to investigate the anti-proliferative effect of Zinc oxide nanosphere was triggered by cell cycle arrest. As shown in Fig. 7B. ZnO nanospheres treatment enhanced the accumulation of the HuH7 cells at the G1/S phase significantly ($P < 0.05$) compared with the control (Fig. 7A). The percentage of the cells at G1/S increased significantly ($P < 0.05$) with increasing ZnO nanospheres concentration. The growth of

the HuH7 treated with ZnO nanospheres was about 42.6 at G1, 11.9, and 45.5% compared to the non-treated cells in which the growth was about 79.8, 16.1, 4.1 %, respectively.

Zinc oxide nanosphere induces apoptosis in Huh7 cells.

As a Fig. 8 revealed a flow cytometric analysis of Zinc oxide nanosphere -induced apoptosis in Huh7 cells using Annexin V-FITC/PI staining. The percentage of the apoptotic cells (including early and late apoptotic cells) increased with increasing concentration of ZnO nanospheres from 8.3 to 39.3% and with time from 6.8 to 38.8 %, Due to the activation of caspase which considered as a hallmark of apoptosis.

Zinc oxide nanosphere induces caspase-dependent apoptosis.

Caspase-3 is one of the executioner caspase members. As Fig. 9 displayed, the data confirmed that Zinc oxide nanosphere activated Caspase – 3 cleavage in a concentration dependent manner.

Quantitative RT-PCR

To investigate the levels of apoptotic genes (p53, Bax Bcl-2, and cytochrome C) in the HuH7 cell after treated with ZnO nanosphere at the concentration of 100 µg/ml for 24 hrs. Data displayed that ZnO nanosphere altered the express genes in HuH7 cells. The mRNA expression level of tumor suppressor gene p53 (Fig. 10A) and pro-apoptotic gene Bax (Fig. 10B), as well as cytochrome (Fig. 10D), were significantly upregulated while the expression of antiapoptotic gene BCL-2 (Fig. 10C) was significantly down-regulated in ZnO NP-treated cells as compared with the untreated control cells (P, 0.05 for each).

Gene expression by flow cytometry

The relative expression of P53, Bax, and Bcl2 has been detected in all treated cells. Treatment of the HuH7 cells with ZnO nanospheres enhanced the relative expression of P53 significantly ($P < 0.05$) by 85% (Fig. 11b). Similarly, it increased the relative expression of Bax and Bcl2 by 65 and 10%, respectively (Fig. 11c). Also, the relative expression of cytochrome C increased in the HuH7 cells treated with ZnO nanospheres by 55% (Fig. 11d) compared to control cells treated with DMSO (Fig. 11a). These findings indicated that ZnO nanospheres regulated the cell cycles *via* stimulating the expression of P53 and Bax genes. The Bcl_2 was less detected than P53 and Bax.

Oxidative stress and antioxidant biomarkers

The primary pathway required to trigger apoptosis mechanistically in a cancerous cell was to induce oxidant generation and antioxidant depletion. Therefore, the oxidants (ROS, LPO, and NO) and antioxidants (GSH and SOD) were studied in the HuH7 cells treated with 100 µg of ZnO nanospheres and Zn II ions (released from100 µg of ZnO nanospheres) after the exposure to 24 hrs. The results illustrated in Figs. 12a, b showed that markers of oxidative stress (ROS and LPO) levels were significantly ($P < 0.05$) higher in the HuH7 cells treated with ZnO nanospheres. As Figs. 12c, d, and e reveled, all the antioxidant

indicators were depleted due to the exposure to both ZnO nanospheres and released Zn II ions. Nevertheless, the released Zn II ions were less than ZnO nanospheres.

Morphological of apoptosis

As Fig. 13 shows, various stages of apoptotic features are appear after HuH7 cell treated with Zinc oxide nanosphere at different time: early stage with" Cup- shaped" chromatin condensation (Fig. 13b), progressive micronuclei formation with plasma membrane –bound apoptotic bodies (Fig. 13c), a secondary necrosis and necrosis as well as swelling and organelle disruption (Fig. 13d) as compared to control cell (Fig. 13a).

Ultrastructure of HuH7 using a transmission electron microscope

TEM analysis of Huh7 cells remedied with Zinc oxide nanosphere at different times demonstrated the typical features of apoptotic cells stages: firstly, rounding up of the cells with disappearance of cytoplasmic as a Fig. (14 b) showed. Secondly, as a time increased, there were many change appearance as a chromatin condensation at the nuclear periphery as Fig. (14 C & D) revealed. Finally, as a Fig. (14 E& F), there is a separation between a two sheets of the nuclear envelope, nuclear fragmentation (a vescicle budded from the nucleus) as compared with control cell in Fig. (14 A). As Fig. (15A) displayed, at high magnification the cytoplasmic vacuoles were droplets. Similarly, other vacuoles with a double membrane existing as Fig. (15B) showed; it mention tht, the mitochondria swelling had occurred as Fig. (15B) showed. Consequently, chromatin condensation associated with mitochondrial swelling as Fig. (15C) displayed. Also, during the apoptosis process, mitochondria tend to conserved till secondary necrosis was carried out as Fig. 14e revealed. Actually, during treatment Hepatoma cell model treated with Zinc oxide nanosphere, number of swollen mitochondria transfer to apoptotic nuclear morphology within an intact plasma membrane.

Discussion

Currently, Nanotechnology has tremendous advancements in the fields of cancer therapy. In recent years, scientists work out to study many inorganic materials with unique properties as effectively, selectively and biocompatibility[38]. Zinc oxide nanomaterial is a popular material due to their unique properties. Based upon their properties, it enters in many applications especially in medical field. Hepatoma classifies as one of the most prevalent malignant diseases in China, Taiwan, Korea, and sub-Saharan Africa[5]. Hepatocellular carcinoma is characterized as a progressive development of preneoplastic and neoplastic lesions[4].

The preparation of zinc oxide nanosphere meets the concept of green chemistry. Green synthesis of nanomaterial is the main topic of material research[39] .This study focused on the construction of zinc oxide nanosphere based on the formation of accumulation of Zinc ion on yeast extract which use as a

bio-template[25]. The plausible mechanism using to fabricate Zinc oxide nanosphere depends on the modified method of sol gel technique. The plausible mechanism for formation zinc oxide nanosphere as the following: The dissolution of zinc acetate in distilled water release zinc ions which accumulate on the outer surface of yeast extract. Therefore, zinc ions reform on a spherical yeast extract. Then, gradually thermal treatment leads to form zinc oxide nanosphere and remove any yeast extract residuals. The physicochemical properties of nanoparticle emphasized that formation of ZnO nanoparticles in spherical shape. ICP is the routine method to evaluate the amount of Zn ions released from suspended ZnO nanosphere. By using MTT assay, Zinc oxide nanosphere is more effective on HuH7 and Vero cells than Zn ions. Furthermore, ZnO nanosphere is more selective to cancerous than normal cell.

Mechanistically, our data revealed that ZnO nanospheres mediated arrest of G1/S phase cell cycle contributed to the inhibition of the HuH7 cell proliferation. Generally, both Cyclin D and cyclin E have an essential role in the progression of the cells *via* a G1 phase of the cell[36]. Also, CDK2 is required during S phase[40]. Annexin V-FITC/PI double-staining assay emphasize the occurrence of apoptosis. Treatment of HuH7 cell with a different concentration as well as different times confirmed that the apoptosis process depends on the activation of caspase which considers as a hallmark of apoptosis[41]. Indeed, caspase results improve that caspase inducing the apoptotic mechanism.

RT-PCR and Flow-cytometry are common techniques to study the molecular mechanism of apoptosis like P53, Bax, Bcl_2, and cytochrome C. there are a couple of mechanisms that meet the concept of apoptosis. The First one is the extrinsic pathway which depends on ligation of a death receptor family Followed by the formation of the death-inducing signaling complex that leading to activation of caspase[42]. The second mechanism is the intrinsic pathway that depends on pro and anti-apoptotic pathways Bcl-2 family proteins. Furthermore, the mitochondrial cytochrome C release facilitates the formation of the apoptosome complex that cleaves and activates the effector caspase[43–44]. Also, there is another approach to induce apoptosis by activated P53 to engage the mitochondria to release cytochrome C.

In current study, treatment of HuH7 cells with ZnO nanosphere increase the pro-oxidant (ROS and LOP). Accorded to Finucane *et al*. (1999) who reported that Zno nanoparticle generate Reactive oxygen species that activate the peroxidation reactions[45]. Also, the elevated ROS level can inflict direct damage to lipids[46]. MDA is considered as a convenient biomarker for peroxidation of omega-3 and omega-6 fatty acids due to their reaction with thiobarbituric acid (TBA) [47]. Similarly, the excessive presence of Zn^{2+} ions triggers harmful oxidative stress. According to Lee *et al*. (2018) who mention that zinc deficiency or excess can cause cellular oxidative stress[48–49]. Hence, liberated zinc ions released from suspended Zinc oxide nanosphere contributed indirectly to stimulating the oxidative stress on HuH7 cell. Moreover, GSH, SOD and NO attenuated the deleterious effect of ROS. GSH represented a major scavenger against ROS. SOD enzyme catalyzes transforming the highly reactive $O^{-}{}_2$ to H_2O_2. Also, NO is a special scavenger against ROS[46].

Transmission electron microscope (TEM) has become a routine method to characterize and describe the inner cell and organelle ultrastructural changes in physiological and pathological conditions[50]. Despite of TEM is the most powerful morphological method to describe apoptosis and necrosis but its images are qualitative and static. So that, the best method to study apoptotic as well as necrotic phenomena should be carried out at different times from its early stage appearance[50].

Apoptosis is a regulated process that control in many pathological and physiological pathways in active manner. It's characterized by various biochemical processes and cascades that make a particular change of the morphology of the cell lading to death of the cell. Multi-factors determine the type of cell termination. The main role of apoptosis is the caspase activation that effect on the level of intracellular ATP. As a result, mitochondria concerned with this type of cell death.

During apoptosis process, the cell shrinks in size and loss contact with adjacent one and losses their surface element such as microvilli and cell- cell linkage. Because of liberation of the cell fluid, the cytoplasm wills condensate leading to changing of the cell volume.as a result, convolution of the nuclear and cellular outlines. Firstly, condensed chromatin tend toward formation cup-shape masses beneath the nuclear envelope to fill thymocytes cells that occupy the mostly of the nuclear volume[51]. Latterly, the apoptosis process will undergoes to a progressive fragmentation leading to forming a number of plasma membrane - bound apoptotic bodies including nuclear and /or cytoplasmic elements[52]. On the other hand, necrosis is another form of cell deletion. In the necrosis process, the plasma membrane will be permeable rapidly. Generally, cell hydration and swelling, as well as organelle disruption appears. Cytosolic components release into extracellular space that leads to respond inflamentary[53]. In contrast of apoptosis, the nucleus shape appears well in the early stages. Transmission electron microscopy analysis of HuH7 cells exposed to zinc oxide nanosphere demonstrated the stages of apoptosis, however, vacuolization was showed. Actually, some of these vacuoles were double-membrane bound vesicles as shown in Fig. 15. These vacuoles include residual cristae structure, may be due to mitochondria swelling. As Fig. 15 reveled cells undergo swelling: the obvious cytoplasmic vacuolization is partially due to the existence of lipid droplets, which lead cells to resemble the characteristic foamy cells observed in the atherosclerotic clots. The reason of vacuolization occurs is absorption of oxidized lipids. Foamy cells are macrophages which have been induced to differentiate by a complex interplay of cytokines, some of them produced by the macrophages themselves (Nagornev *et al.*, 1991)[54]. Also, (Harris& Ralph, 1985) mention that, the apoptotic condition can be inducing cell to differentiate that can be transfer the cell to be a partial differentiation state[55].

Conclusion

Zinc oxide nanoparticle was an important material with a wide range of application in the medical application. Zinc oxide nanosphere increased antioxidant and anti-cancer properties. The transmission microscopy analysis of HuH7 displayed typical features of apoptosis. The overall results showed that

ZnO nanospheres might have some selectivity in their toxic action toward cancer cells, thereby being of potential value as candidate anti-tumor agents

Declarations

Conflict of Interest Statement:

On behalf of all authors, the corresponding author states that there is no conflict of interest.

Acknowledgments

The authors thank Genetic Engineering and Biotechnology Research Institute (GBRI), University of Sadat City, Egypt.

References

1. Bruix, J., Raoul, J. L., Sherman, M., Mazzaferro, V., Bolondi, L., Craxi, A., & Llovet, J. M. (2012). Efficacy and safety of sorafenib in patients with advanced hepatocellular carcinoma: subanalyses of a phase III trial. *Journal of hepatology*, *57*(4), 821-829.
2. Jemal, A., Bray, F., Center, M. M., Ferlay, J., Ward, E., & Forman, D. (2011). Global cancer statistics. *CA: a cancer journal for clinicians*, *61*(2), 69-90.
3. Sawada, Y., Yoshikawa, T., Nobuoka, D., Shirakawa, H., Kuronuma, T., Motomura, Y., & Nakatsura, T. (2012). Phase I trial of a glypican-3–derived peptide vaccine for advanced hepatocellular carcinoma: immunologic evidence and potential for improving overall survival. *Clinical Cancer Research*, *18*(13), 3686-3696.
4. Feo, F.; Simile, M. .; Pascale, R .M. Focal loss of long non-coding RNA-PRAL, as determinant of cell function and phenotype of hepatocellular carcinoma. *Ann Transl Med.***2016**, 4, 9, 183.
5. Ries, LAG.; Melbert, D.; Krapcho, M. SEER Cancer Statistics Review, 1975-2004,National Cancer Institute.Bethesda (MD): **2007**.
6. Nakabayashi, H.; Taketa, K.;Miyano, K.; Yamane, T.; Sato, J. Growth of human hepatoma cells lines with differentiated functions in chemically defined medium. *Cancer Res* **1982**, 42, 3858–3863.
7. Goldring, C.E.; Kitteringham, N.R.; Jenkins, R.; Lovatt, CA; Randle, L.E;. Abdullah A, Owen. A.; Liu, X.; Butler, P.J.; Williams, D.P. Development of a transactivator in hepatoma cells that allows expression of Phase I, Phase II, and chemical defense genes. Am J Physiol Cell Physiol .2006,290,C104–C115.
8. Yoon, H. I., & Seong, J. (2014). Multimodality treatment involving radiotherapy for advanced liver-confined hepatocellular carcinoma. *Oncology*, *87*(Suppl. 1), 90-98.
9. Yeo, W., Mok, T. S., Zee, B., Leung, T. W., Lai, P. B., Lau, W. Y., ... & Johnson, P. J. (2005). A randomized phase III study of doxorubicin versus cisplatin/interferon α-2b/doxorubicin/fluorouracil (PIAF) combination chemotherapy for unresectable hepatocellular carcinoma. *Journal of the National Cancer Institute*, *97*(20), 1532-1538.

10. Gish, R. G., Porta, C., Lazar, L., Ruff, P., Feld, R., Croitoru, A., ... & Kennealey, G. T. (2007). Phase III randomized controlled trial comparing the survival of patients with unresectable hepatocellular carcinoma treated with nolatrexed or doxorubicin. *Journal of clinical oncology*, *25*(21), 3069-3075.
11. Wang, X. Q., Ongkeko, W. M., Chen, L., Yang, Z. F., Lu, P., Chen, K. K., ... & Fan, S. T. (2010). Octamer 4 (Oct4) mediates chemotherapeutic drug resistance in liver cancer cells through a potential Oct4–AKT–ATP-binding cassette G2 pathway. *Hepatology*, *52*(2), 528-539.
12. Ohta, K., Hoshino, H., Hata, K., Wang, J., Huang, S., Menon, V., ... & Hoon, D. S. (2014). MicroRNA mir-93 activates oncogenic c-Met/PI3K/Akt pathway targeting PTEN in hepatocellular carcinoma.
13. Llovet, J. M., & Hernandez-Gea, V. (2014). Hepatocellular carcinoma: reasons for phase III failure and novel perspectives on trial design. *Clinical cancer research*, *20*(8), 2072-2079.
14. Siegel, R., Ward, E., Brawley, O., & Jemal, A. (2011). Cancer statistics, 2011: the impact of eliminating socioeconomic and racial disparities on premature cancer deaths. *CA: a cancer journal for clinicians*, *61*(4), 212-236.
15. Iwamoto, H., Torimura, T., Nakamura, T., Hashimoto, O., Inoue, K., Kurogi, J., & Sata, M. (2011). Metronomic S-1 chemotherapy and vandetanib: an efficacious and non-toxic treatment for hepatocellular carcinoma. *Neoplasia*, *13*(3), 187-197.
16. Peck-Radosavljevic, M. (2014). Drug therapy for advanced-stage liver cancer. *Liver cancer*, *3*(2), 125-131.
17. Wyllie A. H., 1987 - Apoptosis: Cell death in tissue regulation. J.Pathol., 153: 313-316.
18. Mita, P., De Luca, A., Abbro, L., & Dini, L. (2003). Ultrastructural analysis of apoptosis induced by apoptotic U937 cells conditioned medium. *Italian Journal of Zoology*, *70*(2), 141-146
19. An, WG; Kenekal, M.; Simon, M.C.; Maltepe, E.;, Blagosklonny, M.V.;Neckers, LM Stabilization of wild-type p53 by hypoxia- inducible factor 1a.Nature.1998,392,405–408.
1. Fakruddin, M., Hossain, Z., & Afroz, H. (2012). Prospects and applications of nanobiotechnology: a medical perspective. *Journal of nanobiotechnology*, *10*(1), 1-8.
21. Wang, L., Liu, Y., Li, W., Jiang, X., Ji, Y., Wu, X., ... & Chen, C. (2011). Selective targeting of gold nanorods at the mitochondria of cancer cells: implications for cancer therapy. *Nano Letters*, *11*(2), 772-780.
22. Vinardell, M. P., & Mitjans, M. (2015). Anti-tumor activities of metal oxide nanoparticles. *Nanomaterials*, *5*(2), 1004-1021.
23. Look, D. C. (2001). Recent advances in ZnO materials and devices. *Materials Science and Engineering: B*, *80*(1-3), 383-387.
24. Wang, J., Deng, X., Zhang, F., Chen, D., & Ding, W. (2014). ZnO nanoparticle-induced oxidative stress triggers apoptosis by activating JNK signaling pathway in cultured primary astrocytes. *Nanoscale research letters*, *9*(1), 1-12.

1. Bao, S. J., Lei, C., Xu, M. W., Cai, C. J., & Jia, D. Z. (2012). Environment-friendly biomimetic synthesis of TiO2 nanomaterials for photocatalytic application. *Nanotechnology*, *23*(20), 205601.
2. Murdock, R. C., Braydich-Stolle, L., Schrand, A. M., Schlager, J. J., & Hussain, S. M. (2008). Characterization of nanomaterial dispersion in solution prior to in vitro exposure using dynamic light scattering technique. *Toxicological Sciences*, *101*(2), 239-253.
3. Tada-Oikawa, S., Ichihara, G., Suzuki, Y., Izuoka, K., Wu, W., Yamada, Y., & Ichihara, S. (2015). Zn (II) released from zinc oxide nano/microparticles suppresses vasculogenesis in human endothelial colony-forming cells. *Toxicology reports*, *2*, 692-701.

28. Moon, C. S., Zhang, Z. W., Shimbo, S., Akimoto, S., Shimazaki, K., Saito, T., & Ikeda, M. (1996). A comparison of the food composition table-based estimates of dietary element intake with the values obtained by inductively coupled plasma atomic emission spectrometry: an experience in a Japanese population. *Journal of trace elements in medicine and biology*, *10*(4), 237-244.

1. Mossman, T.; Rapid colorimetric assay for cellular growth and survival: application to proliferation and cytotoxicity assays. *J Immunol Meth*.**1983**,65,55–63.
2. Koopman, G., Reutelingsperger, C. P., Kuijten, G. A., Keehnen, R. M., Pals, S. T., & Van Oers, M. H. (1994). Annexin V for flow cytometric detection of phosphatidylserine expression on B cells undergoing apoptosis.
3. Pfaffl, M. W. (2001). A new mathematical model for relative quantification in real-time RT–PCR. *Nucleic acids research*, *29*(9), e45-e45.

1. Clinical significance of bax/bcl-2 ratio in chronic lymphocytic leukemia, Chronic Lymphocytic Leukemia.

1. Al-Shakarchi, W., Alsuraifi, A., Abed, M., Abdullah, M., Richardson, A., Curtis, A., & Hoskins, C. (2018). Combined effect of anticancer agents and cytochrome C decorated hybrid nanoparticles for liver cancer therapy. *Pharmaceutics*, *10*(2), 48.

34. Ohkawa, H., Ohishi, N., & Yagi, K. (1979). Assay for lipid peroxides in animal tissues by thiobarbituric acid reaction. *Analytical Biochemistry*, *95*(2), 351-358.
35. Ellman, G. L. (1959). Tissue sulfhydryl groups. *Archives of biochemistry and biophysics*, *82*(1), 70-77.
36. Green, L. C., Wagner, D. A., Glogowski, J., Skipper, P. L., Wishnok, J. S., & Tannenbaum, S. R. (1982). Analysis of nitrate, nitrite, and [15N] nitrate in biological fluids. *Analytical Biochemistry*, *126*(1), 131-138.

37. Akhtar, M. J., Ahamed, M., Kumar, S., Khan, M. M., Ahmad, J., & Alrokayan, S. A. (2012). Zinc oxide nanoparticles selectively induce apoptosis in human cancer cells through reactive oxygen species. *International journal of nanomedicine*, *7*, 845.
38. Zhang, W.; Meng. J.; Ji, Y.; Li, X.; Kong, H.; Wu, X. Inhibiting metastasis of breast cancer cells in vitro using gold nanorod-siRNA delivery system. Nanoscale.2011,3,3923-32.
39. Qu Y, Kang M, Cheng X andZhao J (2020) Chitosan-Coated Titanium Dioxide-Embedded Paclitaxel Nanoparticles Enhance Anti-Tumor Efficacy Against Osteosarcoma. Front. Oncol. 10:577280. doi: 10.3389/fonc.2020.577280
40. Walker D H, Maller J L. Role for cyclin A in the dependence of mitosis on completion of DNA replication. Nature, 354(6351):314-7, 1991
41. Zhuo, Z. et al. Ailanthone Inhibits Huh7 Cancer Cell Growth via Cell Cycle Arrest and Apoptosis In Vitro and In Vivo. Sci. Rep. 5, 16185; doi: 10.1038/srep16185 (2015).
42. Luo X, Budihardjo I, Zou H, Slaughter C and Wang X. Bid, a Bcl2 interacting protein, mediates cytochrome c release from mitochondria in response to activation of cell surface death receptors. Cell, 94:481-490, 1998.
43. Li H, Zhou H, Xu C J and Yuan J. Cleavage of BID by caspase 8 mediates the mitochondrial damage in the Fas pathway of apoptos. Cell, 94:491-501, 1998.
44. Gross A, Yin X M, Wang K, Wei M C, Jockel J, Milliman C,Erdjument-Bromage H, Tempst P, Korsmeyer S J. Caspase cleaved BID targets mitochondria and is required forcytochrome c release, while BCL-XL prevents this release but not tumor necrosis factor-R1/Fas death. J Biol Chem,274:1156-1163, 1999.
45. Finucane D M, Bossy-Wetzel E, Waterhouse N J, Cotter T G and Green D R. Bax-induced caspase activation and apoptosis via cytochrome c release from mitochondria is inhibitable by BclxL. J Biol Chem, 274:2225-2233, 1999.
46. Moldovan, L.; Moldovan, N. I. Oxygen free radicals and redox biology of organelles. Histochemistry and Cell Biology. 2004, vol. 122, no. 4, pp. 395–412.
47. Schneider, C.; Boeglin, E. W.; Yin, H. Porter, N. A.; Brash, A. R. Intermolecular peroxyl radical reactions during autoxidation of hydroxy and hydroperoxyarachidonic acids generate a novel series of epoxidized products, Chemical Research in Toxicology,2008, 21, 4, 895–903.
48. Sung Ryul Lee. Critical Role of Zinc as Either an Antioxidant or a Prooxidant in Cellular Systems
49. Bai W, Zhang Z, Tian W, He X, Ma Y, Zhao Y, et al. Toxicity of zinc oxide nanoparticles to zebrafish embryo: a physicochemical study of toxicity mechanism. J Nanopart Res. 2009;12: 1645–1654.
50. Burattini S, Ferri P, Battistelli M, Curci R,Luchetti F, Falcieri E (2004) C2C12 murine myoblasts as a model of skeletal muscle development:morpho-functional characterization.Eur J Histochem 48(3):223–233
51. Di Baldassarre A, Secchiero P, Grilli A,Celeghini C, Falcieri E, Zauli G (2000)Morphological features of apoptosis inhematopoietic cells belonging to the T-lymphoid and myeloid lineages. Cell MolBiol 46(1):153–161

52. Falcieri E, Luchetti F, Burattini S, Canonico B,Santi S, Papa S (2000) Lineage-related sensitivityto apoptosis in human tumor cells undergoing hyperthermia. Histochem Cell Biol 113(2):135–144
53. Golstein P, Kroemer G (2007) Cell death by necrosis: towards a molecular de fi nition.Trends Biochem Sci 32(1):37–43
54. Nagornev V. A., Bobryshev Iu. V., Ivanovskii Iu. V., Bogachev Iu. V., 1991 - Role of monocytes-macrophages in atherogenesis. Arkh. Patol., 53: 23-29.
55. Harris P., Ralph P., 1985 - Human leukemic models of myelomonocytic development: a review of the HL-60 and U937 cell lines. J. Leukocyte Biol., 37: 407-422.

Figures

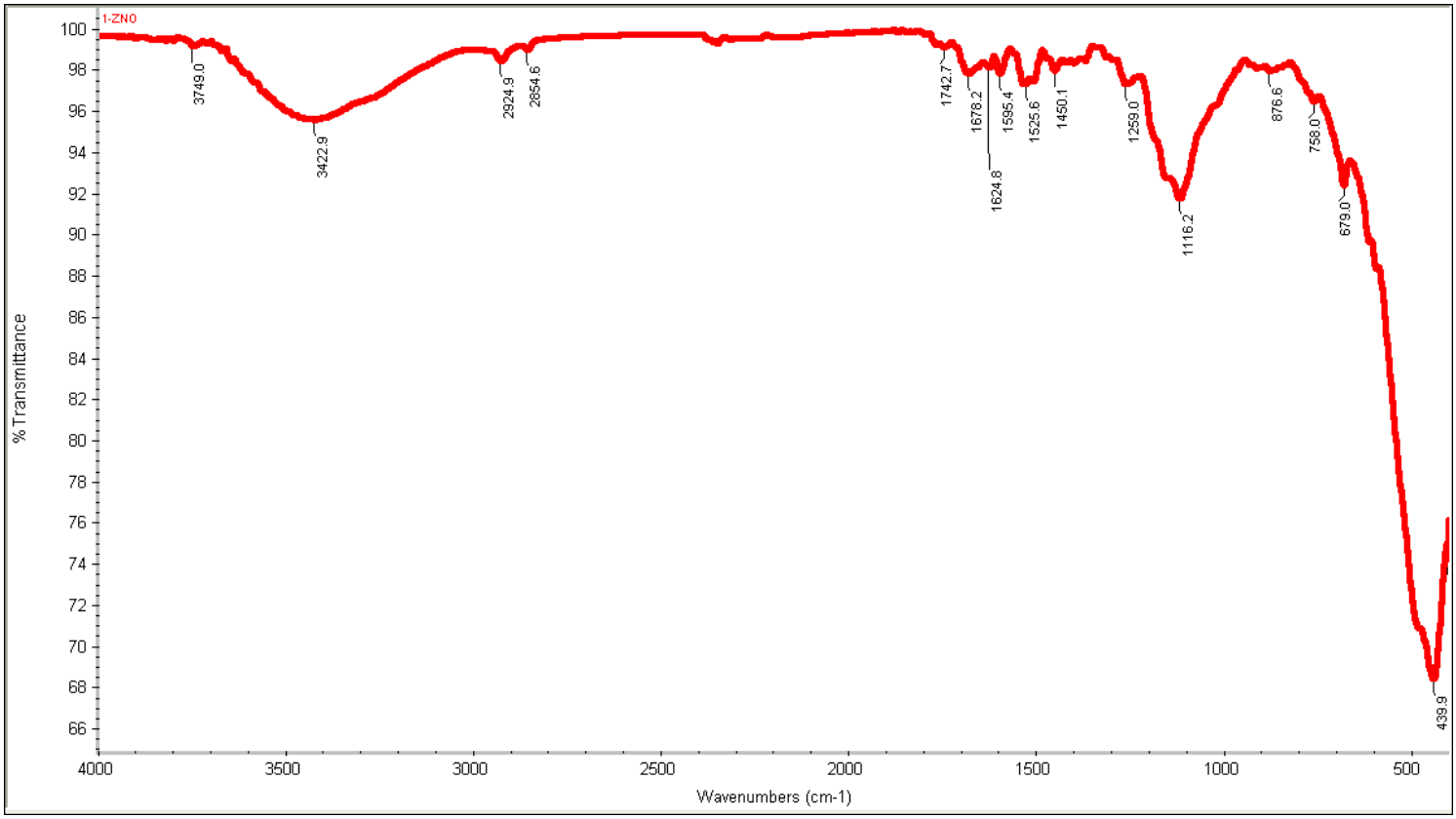

Figure 1

FT-IR spectra ZnO nanospheres (ZnO-NSs).

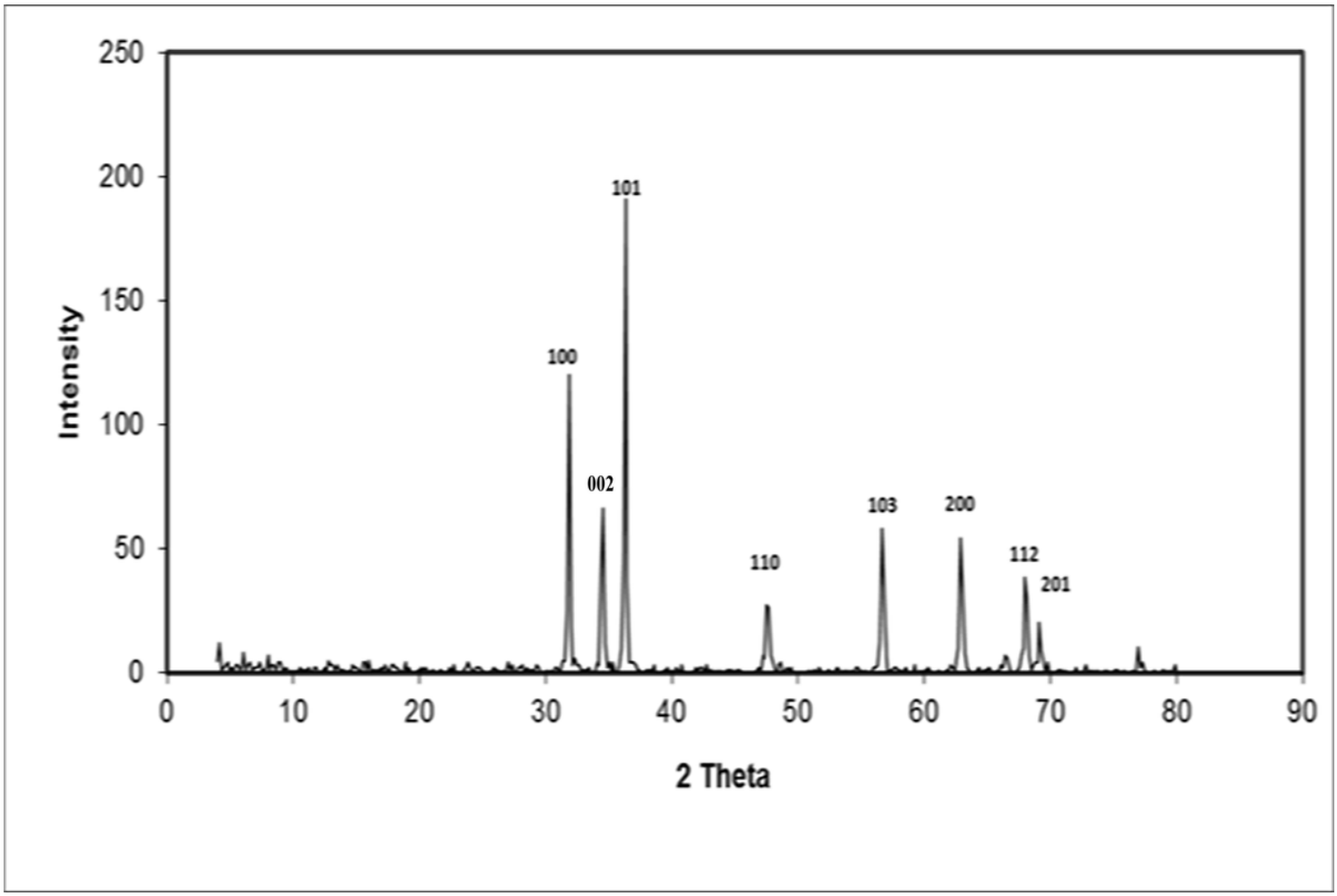

Figure 2

XRD patterns of ZnO nanospheres (ZnO-NSs).

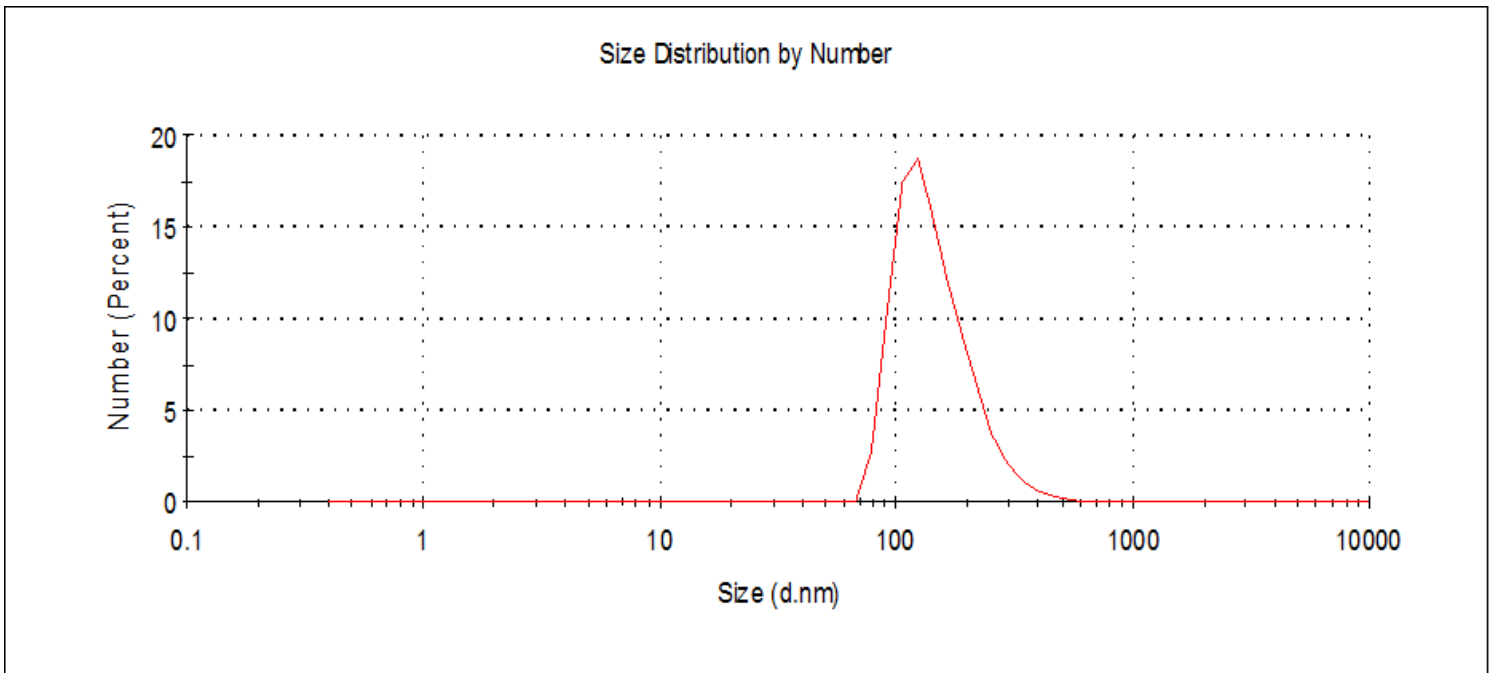

Figure 3

DLS of ZnO nanospheres (ZnO-NSs).

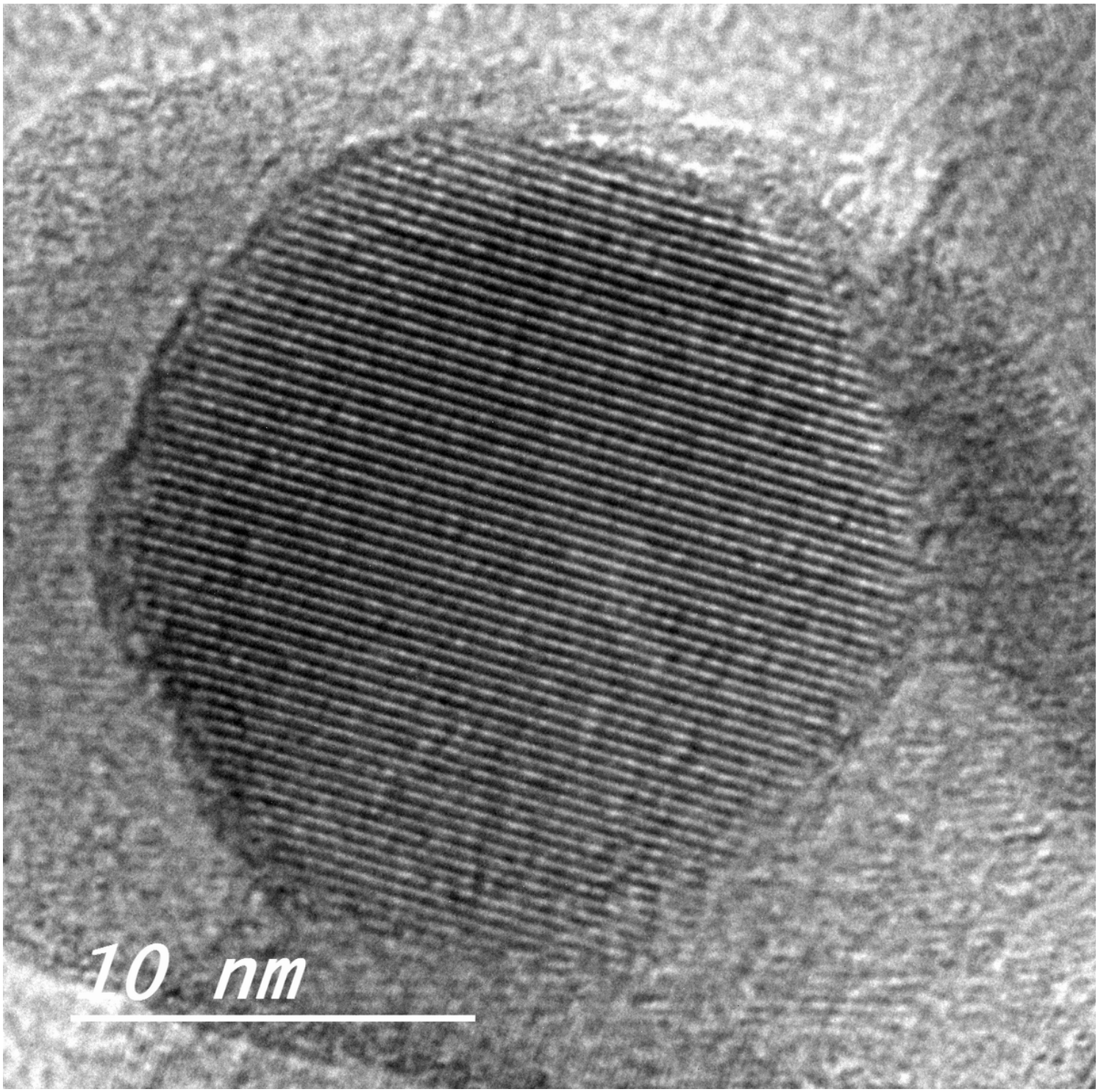

Figure 4

HR-TEM of ZnO nanorods (ZnO-NSs)

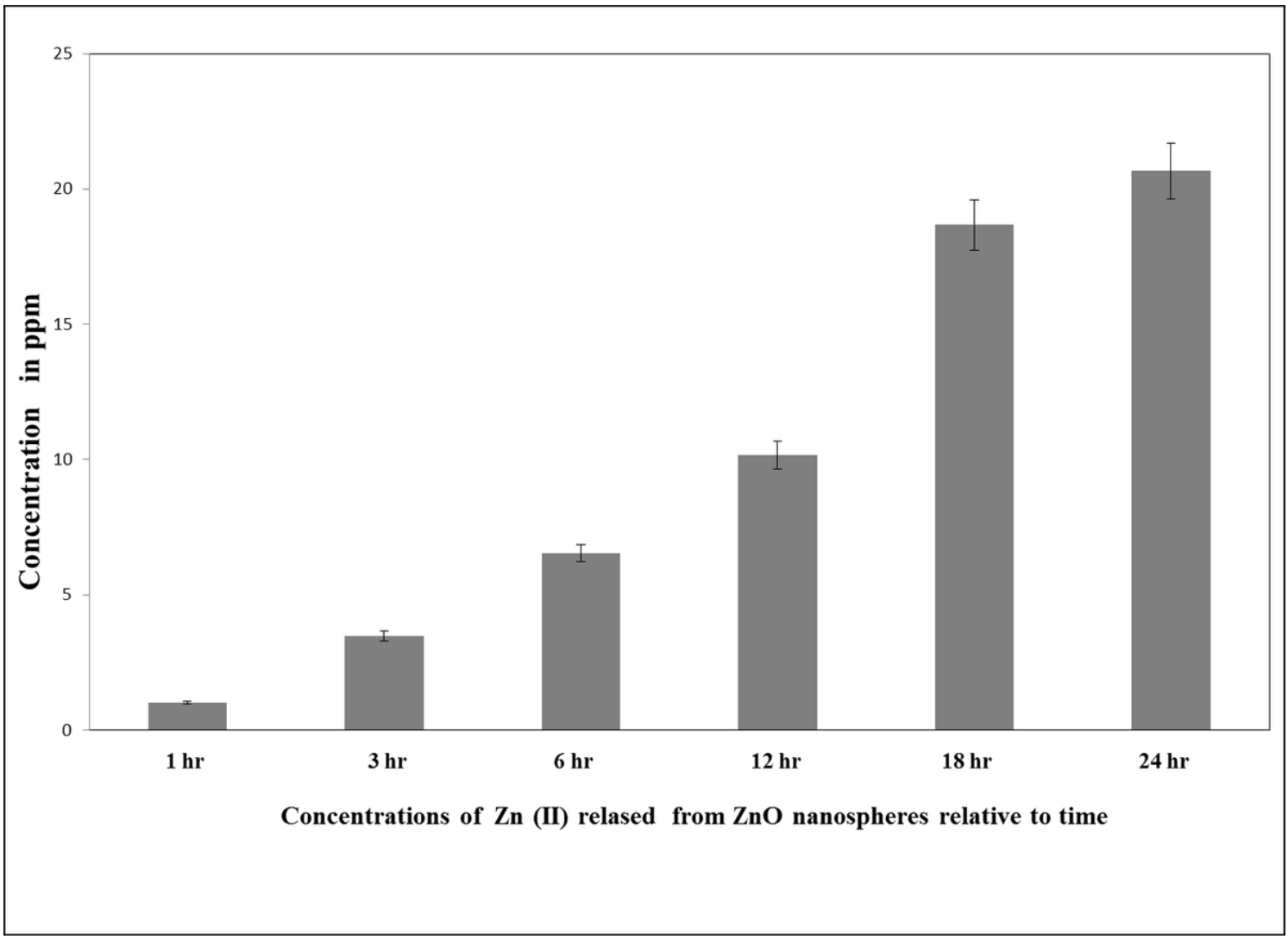

Figure 5

Released Zinc (II) ions from ZnO nanospheres by ICP-AES

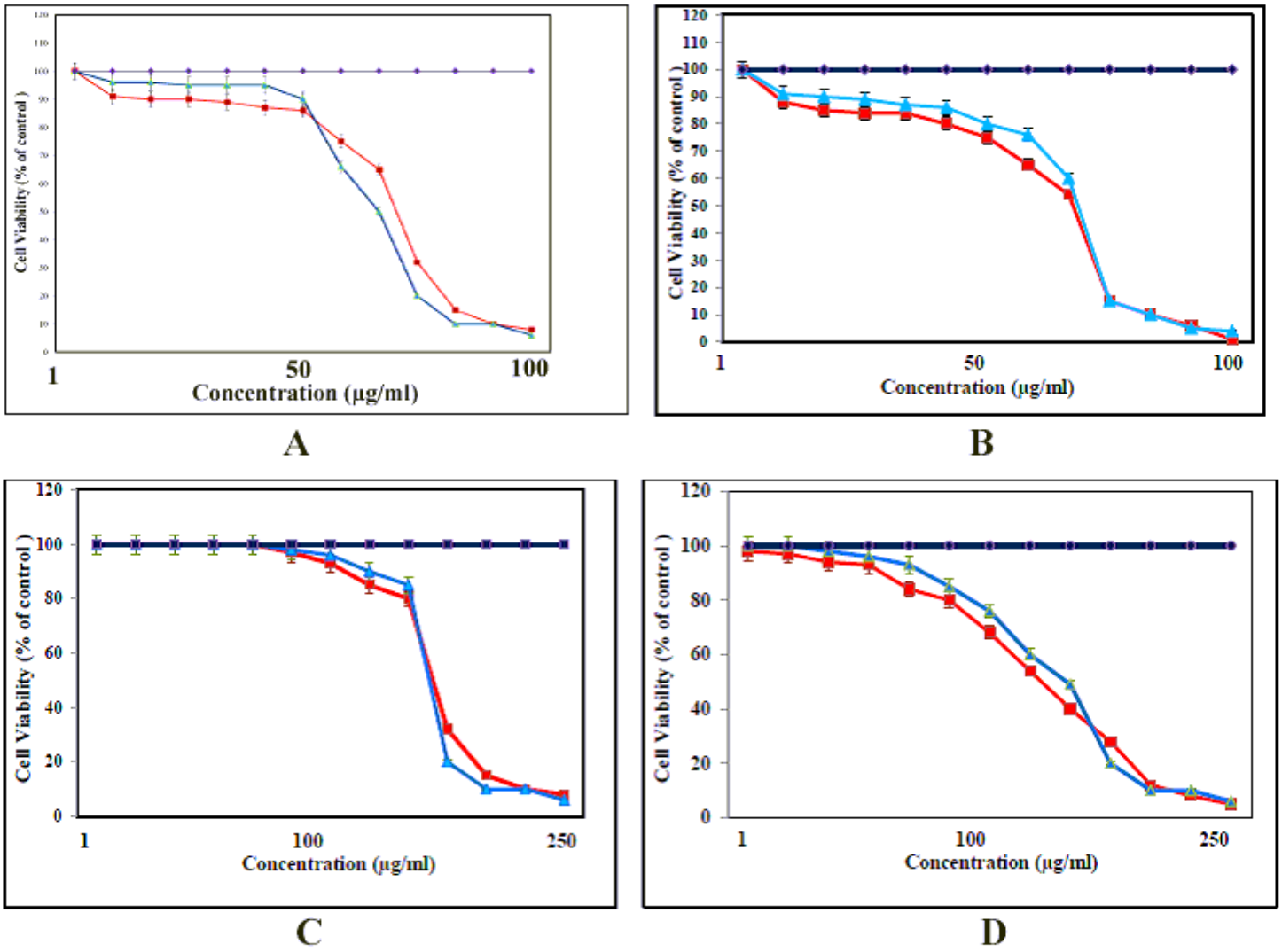

Figure 6

Cytotoxicity effect of ZnO nanospheres and released Zn ion different concentrations on HuH7 cell line with concentrations using MTT assay. . *Statistically significant difference as compared with the controls (P , 0.05 for each). a) Cytotoxicity effect of ZnO nanospheres and released Zn ion different concentrations on HuH7 cell lines with concentrations using MTT assay after 24 hours. b) Cytotoxicity effect of ZnO nanospheres and released Zn ion different concentrations on HuH7 cell line with concentrations using MTT assay after 48 hours. c) Cytotoxicity effect of ZnO nanospheres and released Zn ion different concentrations on Vero cell line with concentrations using MTT assay after 24 hours. d) Cytotoxicity effect of ZnO nanospheres and released Zn ion different concentrations on Vero cell line with concentrations using MTT assay after 48 hours.

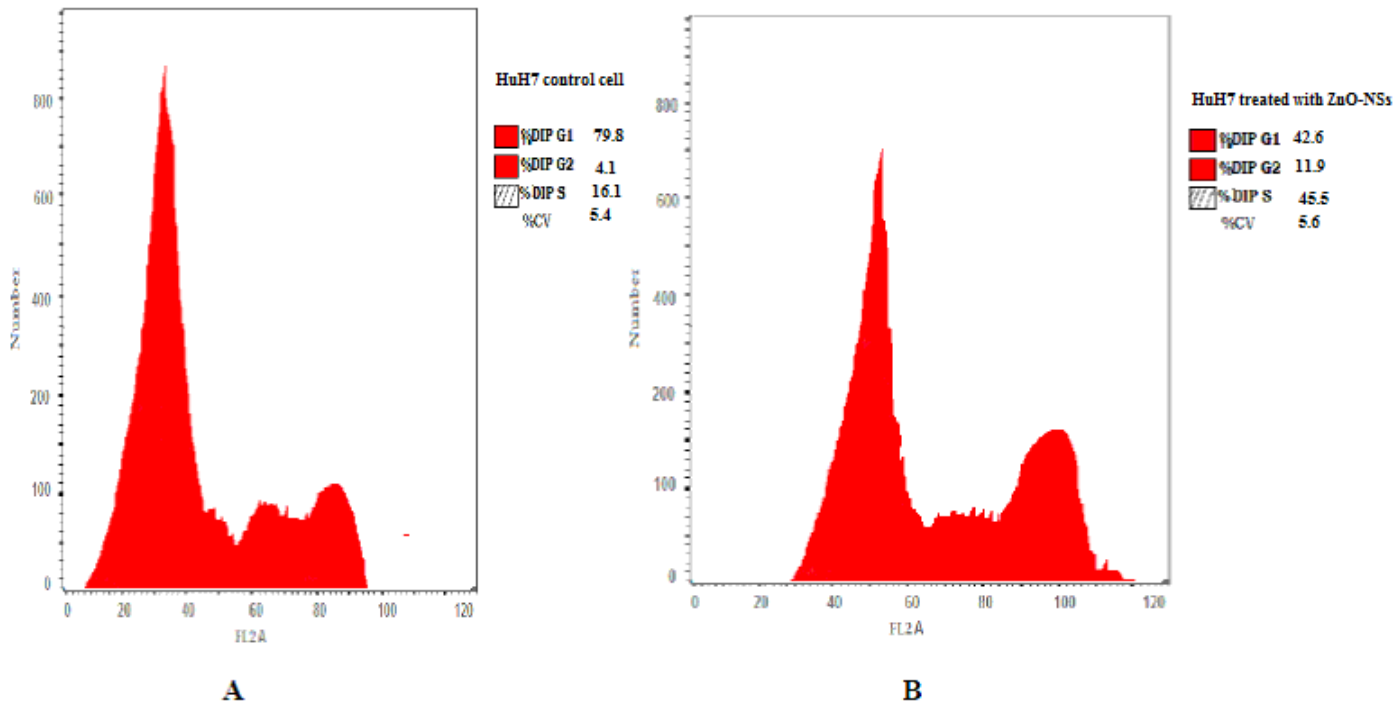

Figure 7

DNA content analysis HuH7 cell line treated with of ZnO nanospheres. a) Negative control (non- treated) b) Treated with 100 µg/ml of ZnO nanospheres (ZnO-NSs)

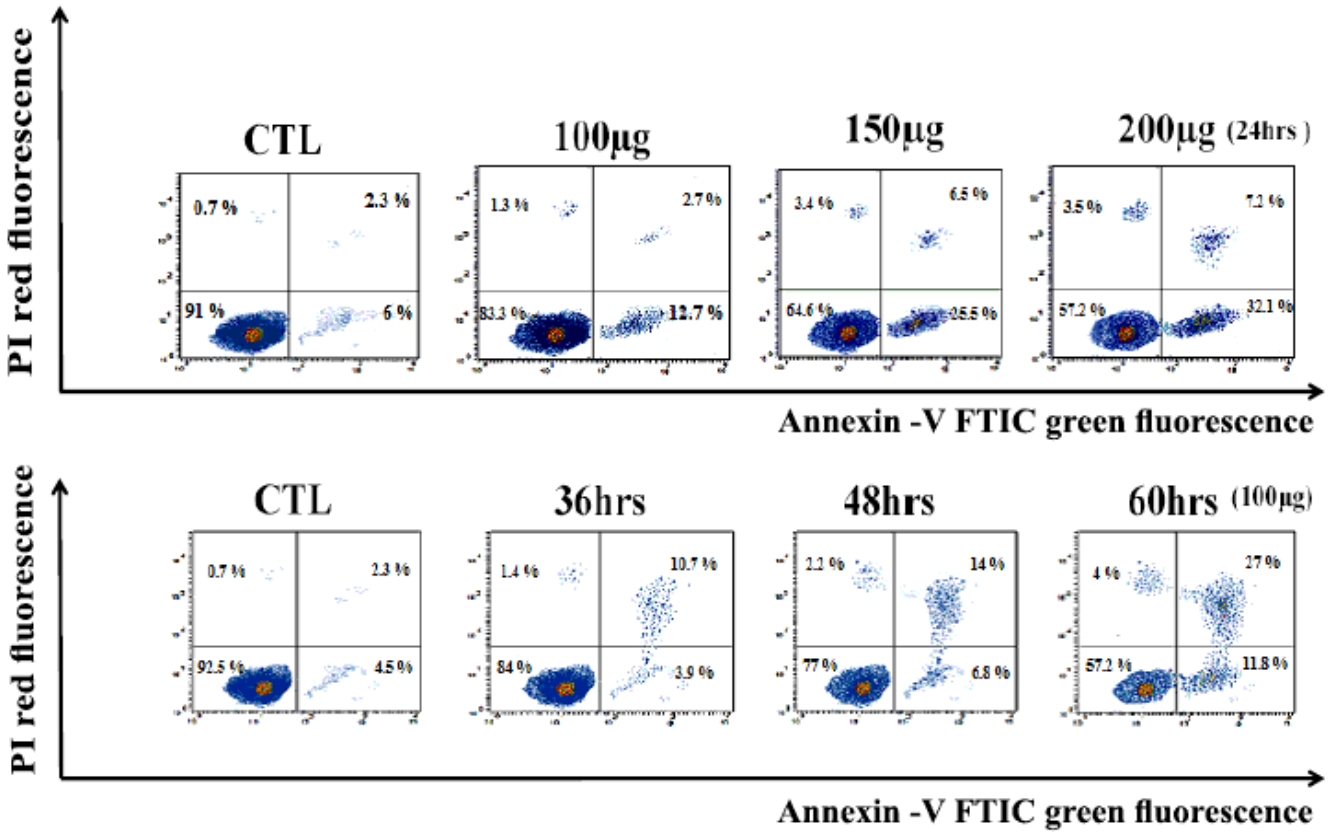

Figure 8

Apoptosis Assay with Annexin V-FITC/PI staining

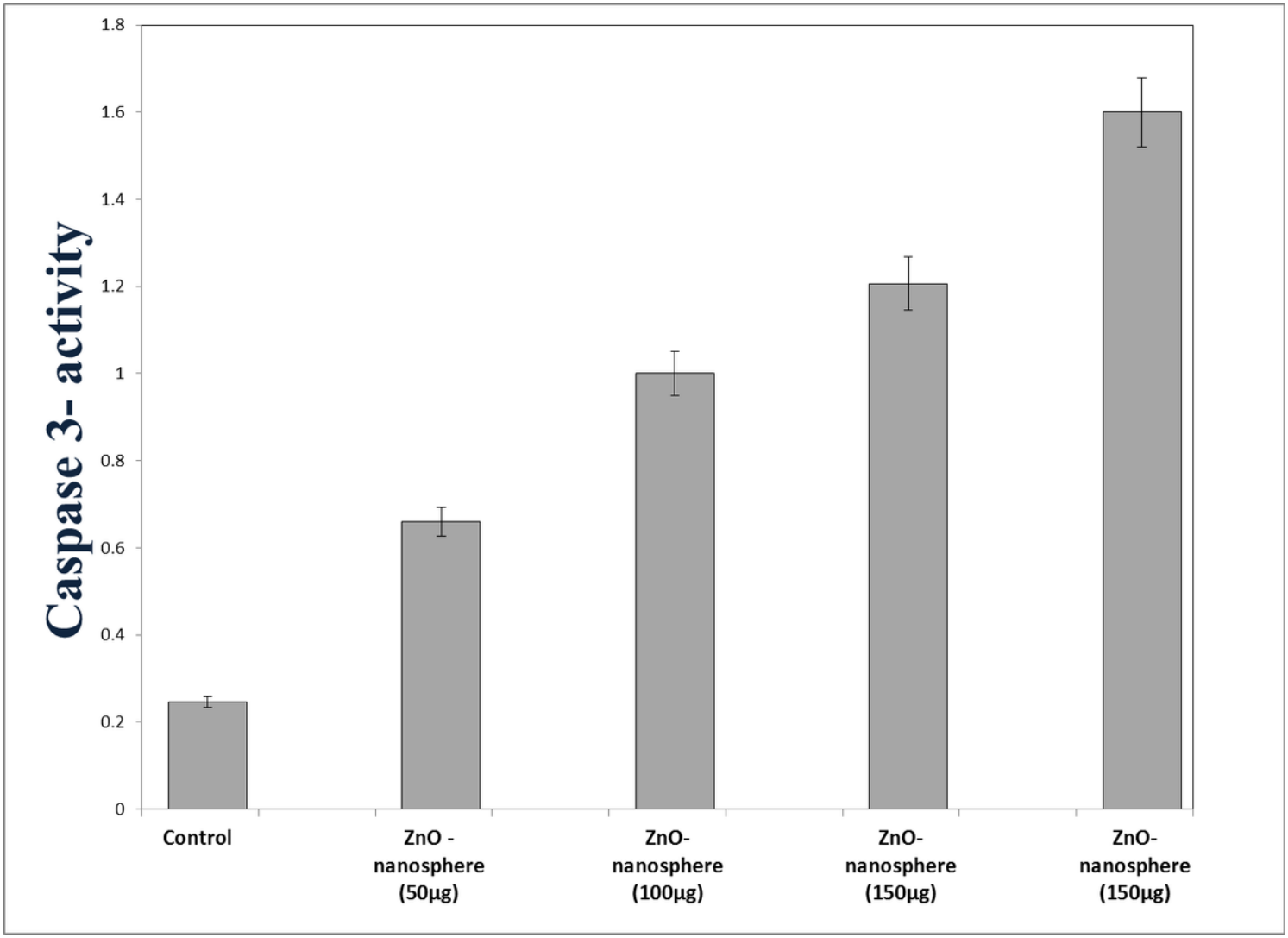

Figure 9

Caspase-3 measurement of ZnO nanospheres. *Statistically significant difference as compared with the controls (P , 0.05 for each).

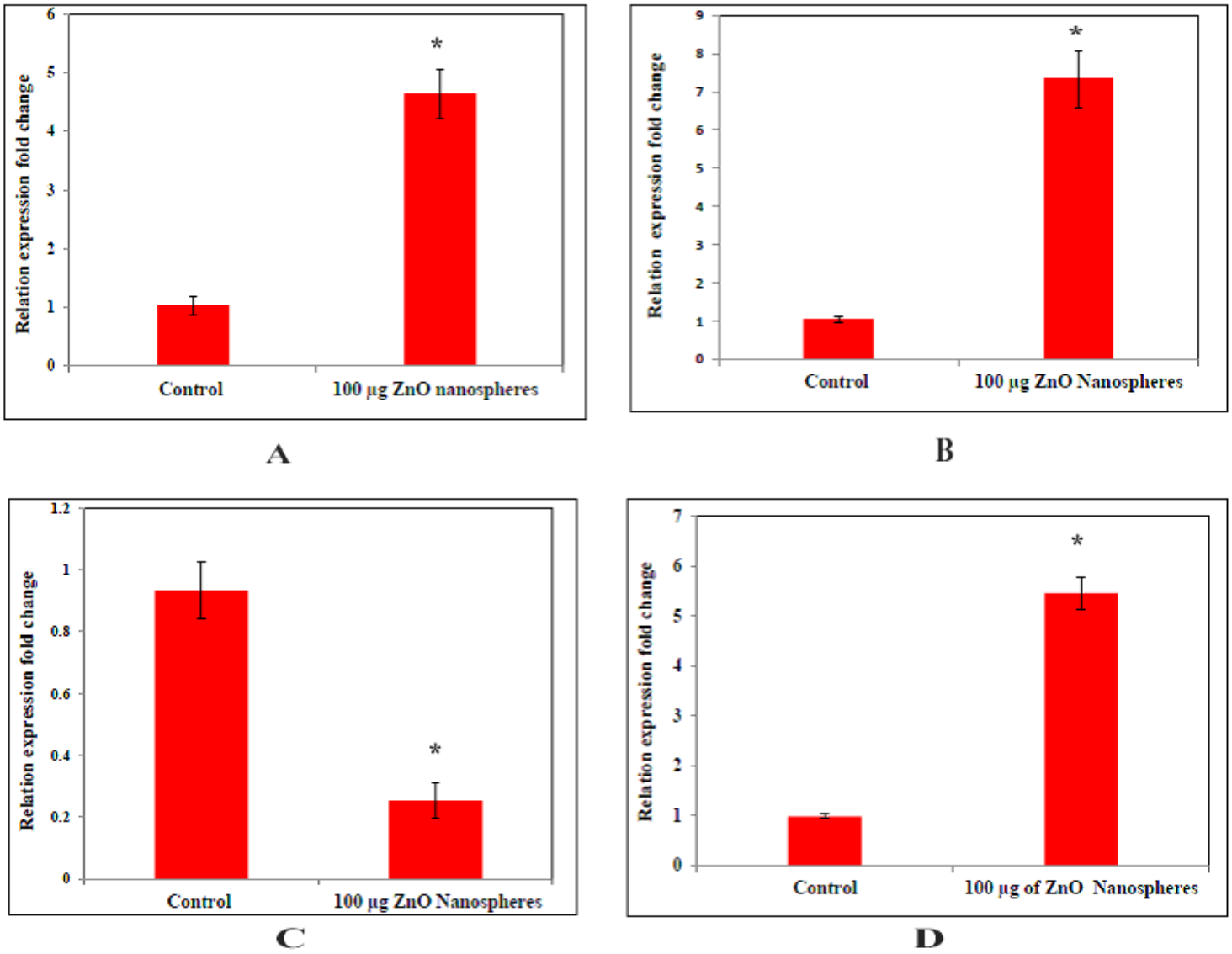

Figure 10

Quantitative real-time PCR measure mRNA levels of HuH7 exposed to100 µg/ml of ZnO nanospheres (ZnO-NSs) for 24 hours .Note: *Statistically significant difference as compared with the controls (P , 0.05for each). a) P53 b) Bax c) Bcl2 d) Cytochrome C

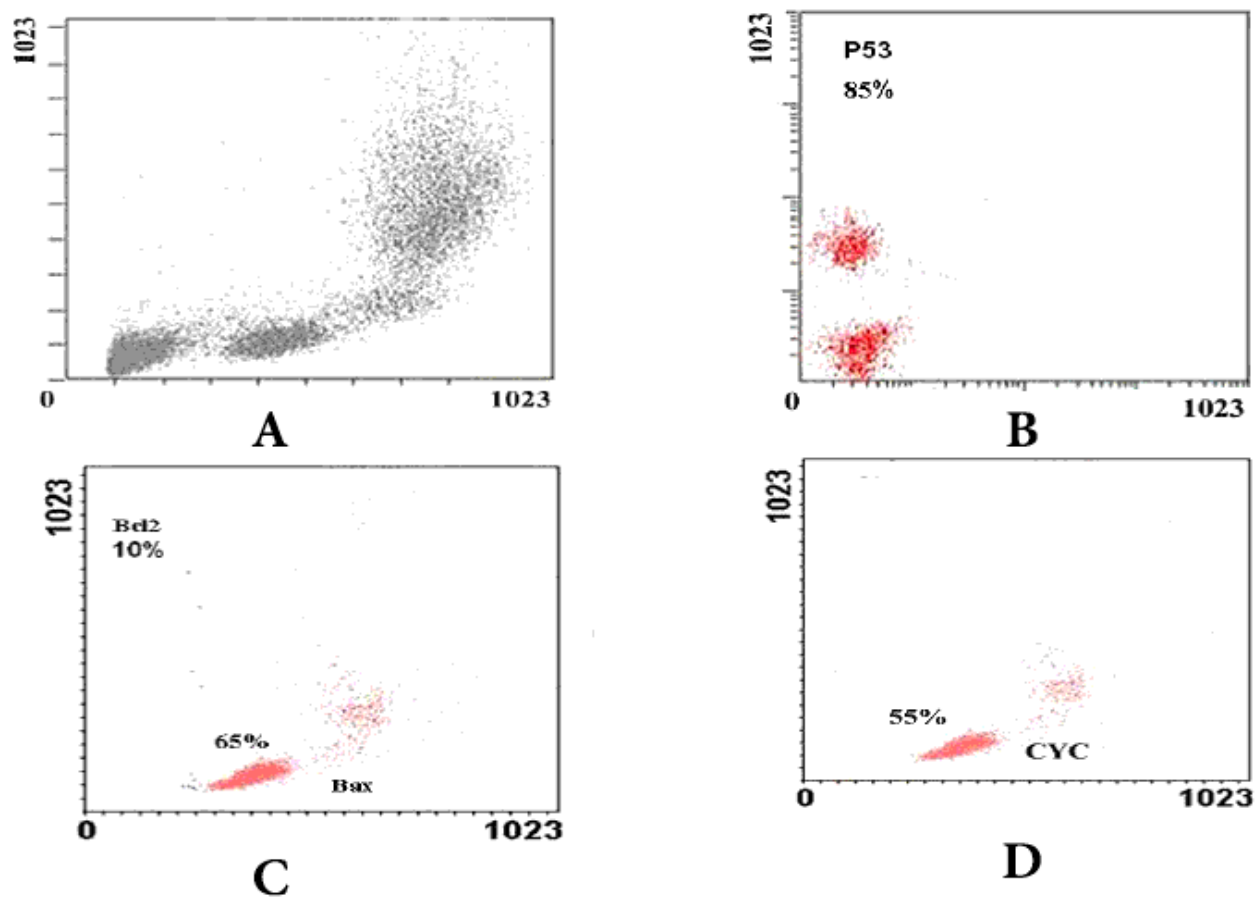

Figure 11

immunoflorescent images of HuH7 exposed to100 µg/ml of ZnO nanospheres (ZnO-NSs) for 24 hours for up-regulation of P53 , Bax , Bcl2 and Cytochrome C. a) The immunoflorescent of huh7 remedied with DMSO b) The immunoflorescent of P53 c) The immunoflorescent of Bax and BcL2 d) The immunoflorescent of Cytochrome C

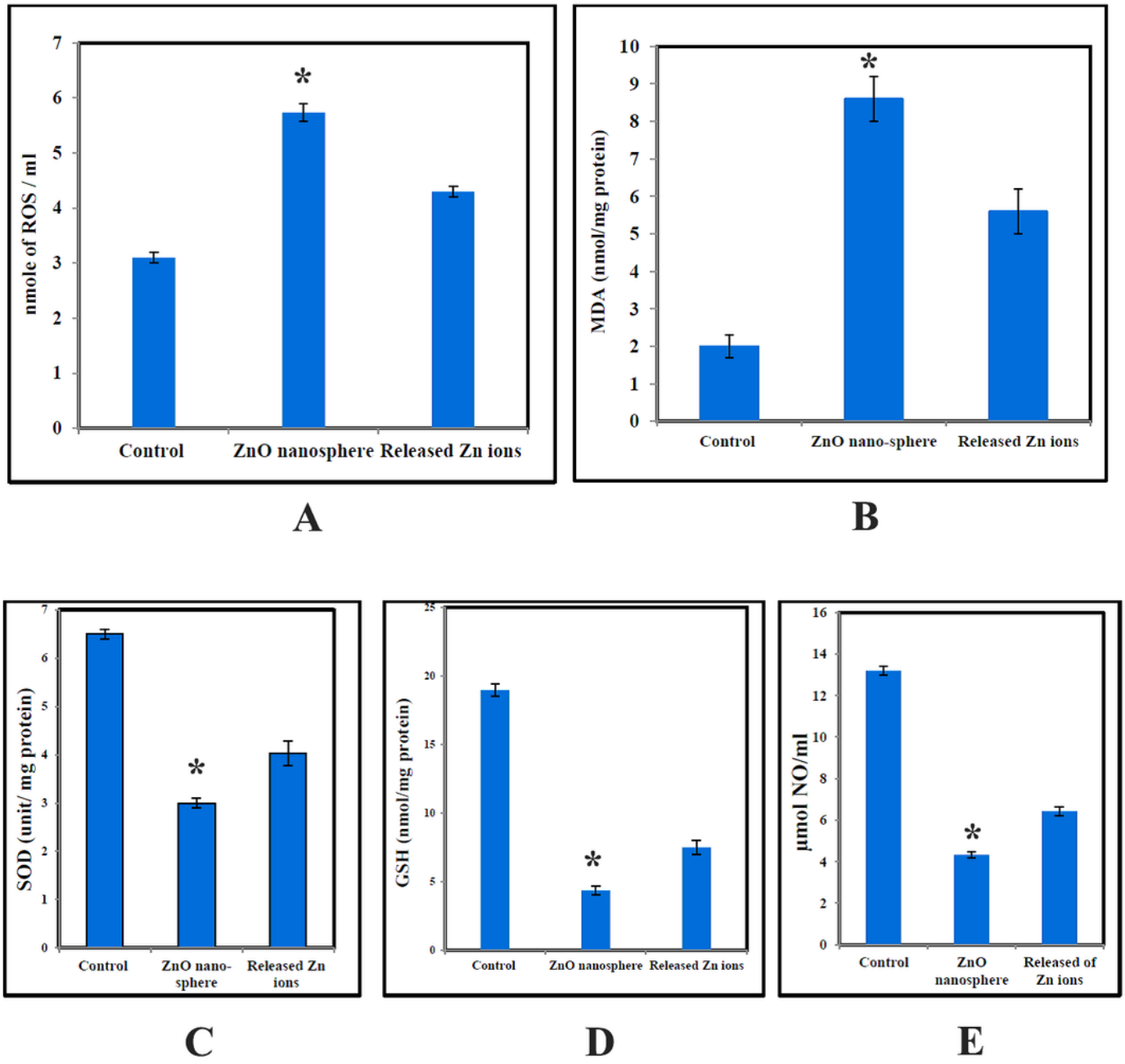

Figure 12

Oxidative stress and antioxidant defense system of human Hepatoma (HuH7) cells after treated with 100 µg/mL ZnO NPs and released Zn ion for 24 hours. Note *Statistically significant difference as compared with the controls (P , 0.05for each). a) ROS b) MDA. c) Glutathione (GSH) d) Superoxide dismutase (SOD) e) Nitric oxide (NO).

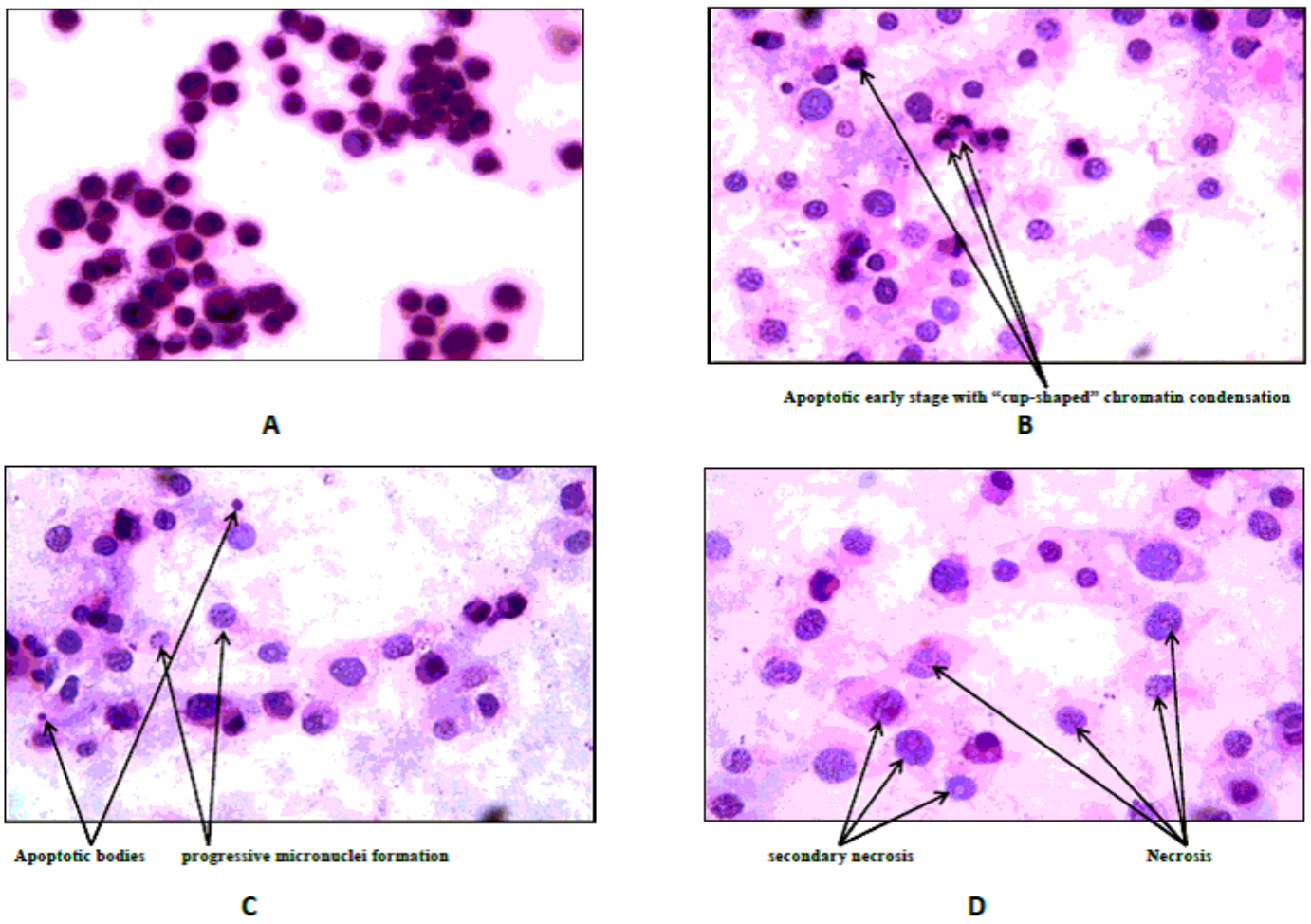

Figure 13

Light micrographs of HuH7cells induced to apoptosis by ZnO-Ns. a) Control HuH7 cell model. b) HuH7 cell after treated with 100 µg ZnO-Ns for 6 hrs. c) HuH7 cell after treated with 100 µg ZnO-Ns for 12 hrs. d) HuH7 cell after treated with 100 µg ZnO-Ns for 24 hrs. *(Original magnification 100X, Oil lens)

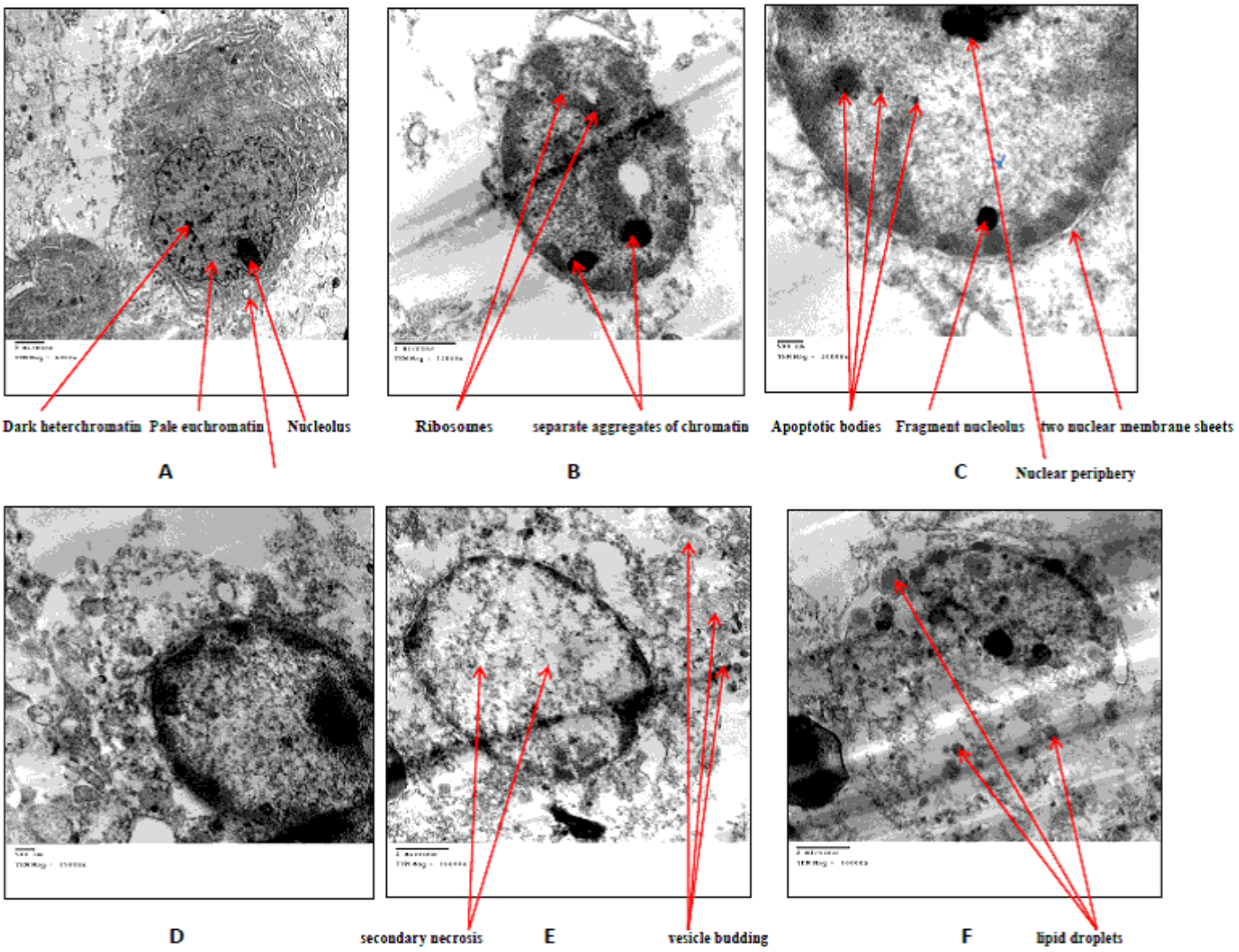

Figure 14

Transmission electron microscope of HuH7 exposed to100 µg/ml of ZnO nanospheres (ZnO-NSs) for 24 hours. a) Control cell b) Treated cell with to100 µg/ml of ZnO nanospheres (ZnO-NSs) for 3 hours. c) Treated cell with to100 µg/ml of ZnO nanospheres (ZnO-NSs) for 6 hours. d) Treated cell with to100 µg/ml of ZnO nanospheres (ZnO-NSs) for 12 hours. e) Treated cell with to100 µg/ml of ZnO nanospheres (ZnO-NSs) for 18 hours. f) Treated cell with to100 µg/ml of ZnO nanospheres (ZnO-NSs) for 24 hours.

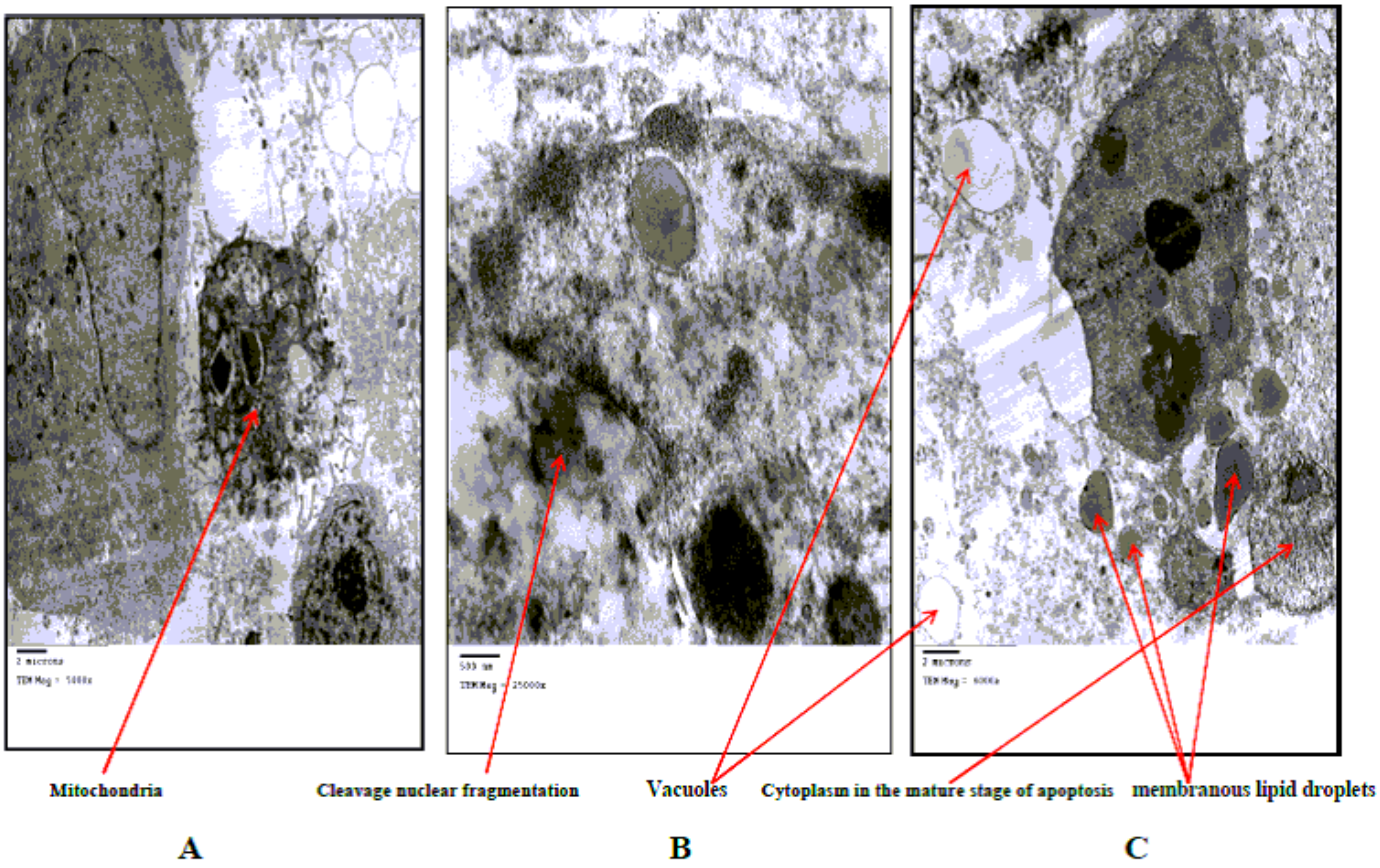

Figure 15

Ultrastructure Analysis of cytoplasmatic vacuolation of HuH7 cells after exposure to ZnO nanospheres. a) HuH7 cell in the mature stage of apoptosis induced by ZnO nanospheres as shown by the cleavage nuclear fragmentation (5,000x). b) HuH7 cell in the early apoptotic stage induced by ZnO nanospheres, as shown by the incomplete chromatin condensation (25,000 x). c) vacuoles are membrane bound, while others are amembranous lipid droplets and cytoplasm in mature stage of apoptosis (6,000x)

Supplementary Files

This is a list of supplementary files associated with this preprint. Click to download.

- S1.UVspectraofZnOnanospheresZnONSs..tif
- S3.HRTEMofZnOnanorodsZnONSs.tif
- Supplementalimagesdoc.docx
- Supplementalimages.docx